Automatic differentiation method for numerical construction of the rotational-vibrational Hamiltonian as a power series in the curvilinear internal coordinates using the Eckart frame

Andrey Yachmenev, and Sergei N. Yurchenko

Citation: J. Chem. Phys. **143**, 014105 (2015); doi: 10.1063/1.4923039
View online: https://doi.org/10.1063/1.4923039
View Table of Contents: http://aip.scitation.org/toc/jcp/143/1
Published by the American Institute of Physics

THE JOURNAL OF CHEMICAL PHYSICS **143**, 014105 (2015)

Automatic differentiation method for numerical construction of the rotational-vibrational Hamiltonian as a power series in the curvilinear internal coordinates using the Eckart frame

Andrey Yachmenev and Sergei N. Yurchenko
Department of Physics and Astronomy, University College London, Gower Street, London WC1E 6BT, United Kingdom

(Received 4 May 2015; accepted 16 June 2015; published online 1 July 2015)

We present a new numerical method to construct a rotational-vibrational Hamiltonian of a general polyatomic molecule in the Eckart frame as a power series expansion in terms of curvilinear internal coordinates. The expansion of the kinetic energy operator of an arbitrary order is obtained numerically using an automatic differentiation (AD) technique. The method is applicable to molecules of arbitrary size and structure and is flexible for choosing various types of internal coordinates. A new way of solving the Eckart-frame equations for curvilinear coordinates also based on the AD technique is presented. The resulting accuracy of the high-order expansion coefficients for the kinetic energy operator using our numerical technique is comparable to that obtained by symbolic differentiation, with the advantage of being faster and less demanding in memory. Examples for H_2CO, NH_3, PH_3, and CH_3Cl molecules demonstrate the advantages of the curvilinear internal coordinates and the Eckart molecular frame for accurate ro-vibrational calculations. Our results show that very high accuracy and quick convergence can be achieved even with moderate expansions if curvilinear coordinates are employed, which is important for applications involving large polyatomic molecules. © *2015 AIP Publishing LLC.* [http://dx.doi.org/10.1063/1.4923039]

I. INTRODUCTION

In recent years, there have been important advances in the development of computational methodologies for an accurate solution of the nuclear motion Schrödinger equation for general medium size polyatomic molecules.[1–10] A growing number of theoretical spectral simulations for atmospheric and astrophysical applications reveal that it is now fairly routine to obtain accurate ro-vibrational energies and spectra for three- and four-atomic molecules (see, for example, Refs. 11–16 for the most recent works), while precise computation of more than five-atomic systems is still a challenging task (see, for example, Refs. 17–24).

The variational method is a widely applied tool for high accuracy ro-vibrational calculations. For large polyatomic molecules, typically with more than three atoms, the variational calculations are computationally excessive due to the essentially exponential scaling of the size of the problem with the number of vibrational degrees of freedom. Although there are powerful methods to conquer this problem such as, for example, various types of basis set contractions, the appropriate choice of the internal coordinates and thus the form of the resulting tailor-made Hamiltonian is a key consideration for their successful application.

Depending on the molecular structure and chosen coordinate system, the task of deriving the expression for the kinetic energy operator (KEO) may be algebraically impossible or require substantial mathematical efforts. The exception is the normal mode coordinates for which the general Watson-type Hamiltonian is available.[25,26] Normal modes, however, are poorly applicable for treating large amplitude motion and high vibrational excitations. Curvilinear coordinates are more physically meaningful and thus are usually considered to be more suitable in these respects.[27] Several types of analytic KEOs in curvilinear internal coordinates have been proposed over the last 30 years by several groups, accompanied by corresponding computer programs, for tri-, four-, and five-atomic molecules using various bond arrangements.[23,28–41] The increasing computer power and great success of quantum chemistry in achieving high accuracy for small and medium size molecules have stimulated recent advances in theoretical spectroscopy towards automatic computational procedures for constructing KEOs that are applicable to molecules with an arbitrary structure and offering user-defined internal coordinates.[1,3,5,42–46]

Another essential advance was the realisation of importance of the Eckart conditions,[47] which are used to define the instantaneous directions of the body-fixed frame such as to minimize the ro-vibrational coupling close to equilibrium. Fulfilling these conditions thus facilitates the basis set convergence of highly excited rotational states. The computational advantages of the Eckart frame embedding have been emphasized in several theoretical studies of the ro-vibrational energies,[10,48–54] spectra,[55] and field-dependent molecular properties.[56] Apart from triatomic[57,58] and planar molecules,[59] it is not possible in general to derive a practicable analytical solution for the Eckart frame equations, instead several numerical approximations have been developed.[60–63] An interesting alternative was recently proposed by

Szalay,[64,65] who suggested to use Cartesian displacement vectors for each atom that simultaneously satisfy the Eckart equations and conditions for defining the internal coordinates. The approach proposed by Dymarsky and Kudin[61] has been very recently implemented in a few ro-vibrational computer codes,[10,53,66] each capable of a numerically exact evaluation of the Eckart conditions in the case of a general molecule. It is noteworthy that the theoretical methods behind these computer programs all belong to a class of approximations that are based on the pointwise, the so-called discrete representations (such as discrete-variable-representation (DVR) methods as well as methods employing quadrature integrations) of the ro-vibrational Hamiltonian at quadrature points, which seems natural considering the numerical character of the Eckart frame solution. In the discrete representation, the KEO is computed numerically exactly at the grid points and therefore is usually called the "exact KEO" approach, although the subsequent matrix elements are approximated with Gaussian quadratures which quickly become impractical or inaccurate if the number of dimensions increases. A number of promising sparse grid methods[67–70] have been recently adapted in the nuclear-motion[71–73] and electronic structure[74] computations to address this issue.

In a different class of approximations, TROVE[3] and a few other methods[29,45,75,76] represent the ro-vibrational Hamiltonian in the product form as a truncated power series in terms of internal coordinates around some fixed or pointwise non-rigid reference configuration. The corresponding KEOs are approximate and often suffer from the round-off and cancellation errors associated with the finite difference approximation used to compute expansion coefficients. Such round-off errors become critical in the case of high-order expansions or high dimensionality. This issue is addressed in the present paper: when resolved we believe that the product form representation approach for the KEO will become more competitive with the discrete representation methods in applications for medium-sized and larger molecules as they are less affected by the so-called curse of dimensionality than the discrete representation methods. Matrix elements in a product basis set can be calculated with very high accuracy even for higher dimensions, since all multivariate integrals are reduced to products of univariate ones.

In this work, we develop a new method of constructing the Eckart-frame KEO as a power series in terms of curvilinear coordinates and implement it as a part of the variational computer program TROVE.[3] The power series expansion of the KEO in TROVE is based on the exact propagation of expansion coefficients from the Cartesian coordinates of atoms to the elements of the kinetic energy matrix and pseudopotential. The expansion coefficients are approximated using finite differences. The approach we propose here forgoes the idea of finite difference derivatives, instead it employs a computer algebra technique called automatic differentiation (AD).[77,78] AD is a numerical technique to evaluate derivatives of an arbitrary order of functions with complex structures defined by computer programs, which are as accurate as if computed using analytically derived derivatives. Unlike finite differentiation, AD does not suffer from the round-off or cancellation errors, and unlike symbolic differentiation it does not lead to expression blow-ups. To adapt the AD tool to our purposes of differentiation of Cartesian coordinates of atoms in the Eckart frame, a two-step procedure is proposed. First, an arbitrary reference coordinate frame is defined such that expressions for Cartesian coordinates become relatively simple analytic functions of internal coordinates. These expressions are converted into a computer code and differentiated by means of the AD tool. To rotate the resulting expansions of the reference-frame Cartesian coordinates into the Eckart frame, they are multiplied, employing the product rules of differential calculus, with the expansion coefficients of the Eckart frame rotation matrix. The latter are obtained in a numerically exact procedure as solutions of the corresponding differentiated Eckart frame equations.

The paper is organized as follows. In Sec. II A, we review the background theory of recursive construction of the power series expansion of the KEO for an arbitrary molecule and internal coordinates. Then, in Secs. II B and II C we present a new approach to construct the expansions of Cartesian coordinates in the Eckart frame. Section II B describes our implementation of AD, while a new method for a numerical solution of the Eckart frame equations is presented in Sec. II C. The expansion of the potential energy and the dipole moment surfaces is discussed in Sec. III. Our algorithm for automatic construction of the product form ro-vibrational Hamiltonian is summarized in Sec. IV. Finally, in Sec. V, examples for four molecules, NH_3, PH_3, H_2CO, and CH_3Cl are given, where we also discuss the convergence properties as well as verify our results against previous highly accurate theoretical calculations.

II. EXPANSION OF THE KINETIC ENERGY OPERATOR

Our approach to build the KEO closely follows the method employed in the variational code TROVE,[3] which attempts a product form representation of the ro-vibrational Hamiltonian by expanding it in power series in terms of internal coordinates. Below, we briefly review the mechanics of this method by building up from a pointwise representation of the KEO to its power series expansion. First, we describe how the power series expansion coefficients of the kinetic energy matrix and pseudopotential may be obtained by exact propagation from the expansion coefficients of Cartesian coordinates of atoms. We then present a new approach for an accurate computation of the power series expansions of Cartesian coordinates in terms of generalized internal coordinates embedded in the Eckart frame.

A. Recursive numerical scheme for the kinetic energy operator

The general form of the ro-vibrational KEO for a molecule with M internal degrees of freedom can be written, in terms of internal coordinates $\boldsymbol{\xi} = \{\xi_1 \ldots \xi_M\}$, as[3]

$$\hat{T} = \frac{1}{2} \sum_{\lambda,\mu=1}^{M+3} p_\lambda^\dagger G_{\lambda\mu}(\boldsymbol{\xi}) p_\mu + U(\boldsymbol{\xi}), \tag{1}$$

where $p_{\lambda=1..M+3} = \{-i\hbar\partial/\partial\xi_1,\ldots,-i\hbar\partial/\partial\xi_M,\hat{J}_x,\hat{J}_y,\hat{J}_z\}$ are the momenta operators conjugate to M internal coordinates as well as three x,y,z components of the total angular momentum operator $\mathbf{J}$. The $M\times M$ and 3×3 blocks of $G_{\lambda\mu}$ are associated with the internal vibrational and overall rotational motions, respectively, while the off-diagonal $M\times 3$ blocks describe coupling between the two motions. The part describing the translational motion of the molecule as a whole is exactly separable from the rotational and internal vibrational motions and is not considered.[3] The kinetic energy matrix $G_{\lambda\mu}(\boldsymbol{\xi})$ and the pseudopotential $U(\boldsymbol{\xi})$, given in general form, are[3,79]

$$G_{\lambda\mu}(\boldsymbol{\xi}) = \sum_i^N \frac{1}{m_i} \sum_{\alpha=x,y,z} s_{\lambda,i\alpha} s_{\mu,i\alpha}, \tag{2}$$

$$U(\boldsymbol{\xi}) = \sum_i^N \frac{1}{m_i} \sum_{\alpha=x,y,z} \sum_{\lambda\mu}^{M+3} \left[\frac{1}{8}[p_\lambda, s_{\lambda,i\alpha}][p_\mu, s_{\mu,i\alpha}] + \frac{1}{4} s_{\lambda,i\alpha}[p_\lambda,[p_\mu, s_{\mu,i\alpha}]] \right], \tag{3}$$

where N denotes the number of nuclei in a molecule and m_i is the mass of the ith nucleus,

$$s_{\lambda,i\alpha} = \frac{\partial\xi_\lambda}{\partial r_{i\alpha}}$$

is the element of the Jacobian matrix. Explicit expressions can be derived for elements of the inverse matrix $\mathbf{t} = \mathbf{s}^{-1}$, given by[79]

$$t_{i\alpha,k} = \frac{\partial r_{i\alpha}}{\partial\xi_k} \quad (k = 1,\ldots,M), \tag{4}$$

$$t_{i\alpha,M+\beta} = \sum_{\gamma=x,y,z} \epsilon_{\alpha\beta\gamma} r_{i\gamma} \quad (\beta = x,y,z), \tag{5}$$

$$t_{i\alpha,M+3+\beta} = \delta_{\alpha\beta} \quad (\beta = x,y,z), \tag{6}$$

where $r_{i\alpha}$ denotes a Cartesian component ($\alpha = x,y,z$) of an ith nucleus, $\epsilon_{\alpha\beta\gamma}$ is the Levi-Civita symbol, and $t_{i\alpha,k}$, $t_{i\alpha,M+\beta}$ and $t_{i\alpha,M+3+\beta}$ are identified with the M vibrational, three rotational, and three translational coordinates, respectively. The computation of the matrix $\mathbf{s}$ is a straightforward matter of inverting the matrix $\mathbf{t}$, which is equivalent to solving a $3N \times 3N$ system of linear equations simultaneously for $3N$ right-hand side vectors,[3] as defined by

$$\sum_i^N \sum_{\alpha=x,y,z} s_{\lambda,i\alpha}\, t_{i\alpha,\mu} = \delta_{\lambda\mu} \quad (\lambda,\mu = 1,\ldots,3N). \tag{7}$$

In Eqs. (4) and (5), the explicit expressions for Cartesian coordinates $r_{i\alpha}$ and their derivatives $\partial r_{i\alpha}/\partial\xi_k$ as functions of internal coordinates ξ_k are specific to the number and arrangement of bonds in the molecule, the definition of internal coordinates, as well as the relative orientation of the body-fixed axes in a molecule. As internal coordinates, one can choose any coordinates that unambiguously define the relative instantaneous positions of the nuclei. Examples are normal coordinates, linearized or curvilinear internal displacement coordinates (displacements of bond lengths, bond angles, dihedral angles from their respective equilibrium values), symmetry-adapted linear combinations of them, etc.

Among the methods commonly used to define the orientation of the body-fixed axes for an arbitrary instantaneous configuration, required for the three conditions in Eq. (5), are the well known Z-matrix representation, a molecular bond frame, the Eckart[29,47] and principal axes systems (PAS). As an example of a molecular bond frame, for the ammonia molecule one can choose the z-axis to be always directing along the trisector vector and the y-axis along one of the bond projections on a plane perpendicular to z. The Eckart and PAS frames are used to relax the orientation of the frame axes with respect to variations of the internal coordinates and to minimize the ro-vibrational coupling terms in the KEO by satisfying certain conditions, which we discuss in detail below.

The Eckart and PAS conditions can be conveniently formulated in terms of a 3×3 orthogonal matrix $\mathbf{d}(\boldsymbol{\xi})$ describing a rotation of the Cartesian coordinates from some reference into the Eckart or PAS frames as given by

$$r_{i\alpha}(\boldsymbol{\xi}) = \sum_{\beta=x,y,z} d_{\alpha\beta}(\boldsymbol{\xi})\bar{r}_{i\beta}(\boldsymbol{\xi}), \tag{8}$$

where $\bar{r}_{i\beta}$ and $r_{i\alpha}$ denote Cartesian coordinates of atoms in the reference and Eckart (or PAS) frames, respectively. The Eckart conditions are based on the equilibrium molecular configuration $r_{i\alpha}^{(\mathrm{eq})}$ and can be formulated in terms of the rotation matrix $\mathbf{d}(\boldsymbol{\xi})$ by

$$\mathbf{u}\mathbf{d}^T - \mathbf{d}\mathbf{u}^T = 0, \tag{9}$$

$$u_{\alpha\beta} = \sum_i^N m_i r_{i\alpha}^{(\mathrm{eq})}\bar{r}_{i\beta}, \tag{10}$$

where m_i is the mass of the ith nucleus. The equilibrium values $r_{i\alpha}^{(\mathrm{eq})}$ are usually obtained from the values of internal coordinates corresponding to the minimum of the PES.

Note that we distinguish the frame in which the equilibrium Cartesian coordinates are defined (Eq. (10)) and the instantaneous reference frame (Eq. (8)). For example, a convenient choice for the reference frame is the Z-matrix or molecular bond frame, discussed above. The standard choice for the equilibrium configuration $r_{i\alpha}^{(\mathrm{eq})}$ is the PAS frame,[3,29] which leads to efficient decoupling in the pure rotational part of the KEO. As we will show in Sec. II C, choosing the equilibrium configuration $r_{i\alpha}^{(\mathrm{eq})}$ in the reference frame simplifies the expansion of the Eckart equations.

Using the reference frame, the PAS conditions take the form

$$[\mathbf{d}\tilde{\mathbf{u}}\mathbf{d}^T]_{\alpha\beta} = 0 \quad \alpha \neq \beta, \tag{11}$$

$$\tilde{u}_{\alpha\beta} = \sum_i^N m_i \bar{r}_{i\alpha}\bar{r}_{i\beta}, \tag{12}$$

which, in contrast to the Eckart frame, does not depend on the equilibrium structure and thus may become preferable in cases where the latter is not well defined.

With the exception of triatomic[57,58] and planar molecules,[59] i.e., when one of the axes' directions is fixed, it is not possible to derive a closed-form analytical solution of the Eckart equations, instead several numerical approximations have been introduced.[60–62] The numerical procedure of

Dymarsky and Kudin[61] has been recently adapted in several nuclear-motion computational models,[10,53,66] each of which employs a discrete representation of the ro-vibrational Hamiltonian and evaluates the Eckart-frame KEO at grid points. Further, in Sec. II C we propose an alternative method for numerical solution of the Eckart equations as a power series expansion in terms of internal coordinates.

The methodology to construct the KEO presented above can be directly applied to compute the KEO at a given discrete point, especially useful when the quadrature integrations or DVR methods are employed. The methodology can also be easily extended for the KEOs in the product-form power series representation. Following the TROVE approach[3] we write all quantities in Eqs. (2)–(7) as finite-order polynomials in the internal coordinates, as given by

$$G_{\lambda\mu}(\boldsymbol{\xi}) = \sum_{0\le|\mathbf{l}|\le L} g_{\mathbf{l}}^{(\lambda\mu)} \xi_1^{l_1} \dots \xi_M^{l_M}, \tag{13}$$

$$s_{\lambda,i\alpha}(\boldsymbol{\xi}) = \sum_{0\le|\mathbf{l}|\le L} s_{\mathbf{l}}^{(\lambda,i\alpha)} \xi_1^{l_1} \dots \xi_M^{l_M}, \tag{14}$$

where $\mathbf{l} = \{l_1, \dots, l_M\}$ denotes an M-dimensional multi-index defining the order of partial derivatives, and $g_{\mathbf{l}}^{(\lambda\mu)}$ and $s_{\mathbf{l}}^{(\lambda,i\alpha)}$ denote the corresponding expansion coefficients. The analogous expressions can also be written for $U(\boldsymbol{\xi})$ and $t_{i\alpha,\lambda}(\boldsymbol{\xi})$. The expansions sum over all multi-indexes $\mathbf{l} \in \mathbb{N}^M$ with the norm $|\mathbf{l}|$ less or equal to the respective maximal expansion order L. Using the above definitions and applying the generalized Leibniz product rule,[80] the basic expressions in Eqs. (2) and (7) can be rewritten in terms of the expansion coefficients as

$$g_{\mathbf{l}}^{(\lambda\mu)} = \sum_{\substack{\mathbf{0}\le\mathbf{k}\le\mathbf{l} \\ \mathbf{k}\in\mathbb{N}^M}} \sum_{i}^{N} \frac{1}{m_i} \sum_{\alpha=x,y,z} s_{\mathbf{k}}^{(\lambda,i\alpha)} s_{\mathbf{l}-\mathbf{k}}^{(\mu,i\alpha)}, \tag{15}$$

$$\sum_{i,\alpha} s_{\mathbf{l}}^{(\lambda,i\alpha)} t_{\mathbf{0}}^{(i\alpha,\mu)} = \delta_{\lambda\mu}\delta_{\mathbf{l}\mathbf{0}} - \sum_{\substack{\mathbf{0}\le\mathbf{k}<\mathbf{l} \\ \mathbf{k}\in\mathbb{N}^M}} \sum_{i,\alpha} s_{\mathbf{k}}^{(\lambda,i\alpha)} t_{\mathbf{l}-\mathbf{k}}^{(i\alpha,\mu)}, \tag{16}$$

where we avoid giving the expression for the pseudopotential as too burdensome (see Ref. 3 for details). In these equations, $\mathbf{l}$ and $\mathbf{k}$ are multi-indexes, $t_{\mathbf{l}}^{(i\alpha,\mu)}$ are the expansion coefficients of the $\mathbf{t}$ matrix, and $\mathbf{0} = \{0, \dots, 0_M\}$ denotes the zero-order expansion term. From Eq. (15), it follows that the Lth order expansion of the $G_{\lambda\mu}$ matrix can be constructed from the same order expansions of $\mathbf{s}_\lambda$ and $\mathbf{s}_\mu$. For the Lth order expansion of the pseudopotential, however, up to the $(L+2)$-order expansion terms of $\mathbf{s}$ are required, as follows from Eq. (3) or more evidently from Eq. (31) of Ref. 3. The expansion coefficients $s_{\mathbf{l}}^{(\lambda,i\alpha)}$ are evaluated from $t_{\mathbf{l}}^{(\lambda,i\alpha)}$ using Eq. (16). For each expansion coefficient $s_{\mathbf{l}}^{(\lambda,i\alpha)}$ of the order given by the multi-index $\mathbf{l}$, we arrive to a system of linear equations with the right hand side vector containing a sum over all coefficients of an order lower than $\mathbf{l}$ and the linear system matrix given by the elements of the matrix $t_{\mathbf{0}}^{(i\alpha,\mu)} \equiv t_{i\alpha,\mu}$. The latter is common for all linear equations on $s_{\mathbf{l}}^{(\lambda,i\alpha)}$, thus its inverse is computed once and subsequently used to obtain all solutions. Hence, all high-order expansion coefficients $s_{\mathbf{l}}^{(\lambda,i\alpha)}$ may be generated recursively starting from the coefficients of lower orders. As it follows from Eqs. (4) and (5), the coefficients $t_{\mathbf{l}}^{(i\alpha,\mu)}$ are related to the derivatives of the Cartesian coordinates $r_{i\alpha}(\boldsymbol{\xi})$ via

$$t_{\mathbf{l}}^{(i\alpha,k)} = \frac{1}{|\mathbf{l}|!(l_k+1)} \left.\frac{\partial^{|\mathbf{l}|+1} r_{i\alpha}}{\partial\xi_1^{l_1}\dots\partial\xi_k^{l_k+1}\dots\partial\xi_M^{l_M}}\right|_{\boldsymbol{\xi}=0} \quad (k = 1,\dots,M), \tag{17}$$

$$t_{\mathbf{l}}^{(i\alpha,M+\beta)} = \frac{1}{|\mathbf{l}|!} \sum_{\gamma=x,y,z} \epsilon_{\alpha\beta\gamma} \left.\frac{\partial^{|\mathbf{l}|} r_{i\gamma}}{\partial\xi_1^{l_1}\dots\partial\xi_M^{l_M}}\right|_{\boldsymbol{\xi}=0} \quad (\beta = x,y,z). \tag{18}$$

Thus, coefficients $t_{\mathbf{l}}^{(i\alpha,\mu)}$, and therefore the coefficients $s_{\mathbf{l}}^{(\lambda,i\alpha)}$ and $g_{\mathbf{l}}^{(\lambda,\mu)}$ can all be obtained from the derivatives of the Cartesian coordinates $r_{i\alpha}(\boldsymbol{\xi})$, whose accurate computation is the central topic of this paper and is the focus of Secs. II B and II C.

Before describing our new method for computing derivatives of Cartesian coordinates, some remarks should be made about the existing approximations. One of the most popular and universal approaches to compute arbitrary order partial derivatives of a general function is to use central finite differences, also employed by TROVE.[3] For derivatives of Cartesian coordinates this means that one must numerically solve the Eckart equations (Eq. (9)) and compute the Eckart-frame Cartesian coordinates (Eq. (8)) at each finite step in the internal coordinates. Despite its straightforward formulation and ease of implementation, the finite difference method has several drawbacks. The most significant are the round-off and cancellation errors caused by the finite step size as well as the rapidly growing number of finite steps if high-order derivatives or partial derivatives with respect to too many variables (for larger molecules) are concerned. The use of the quadrupole-precision floating-point numbers[3] and more accurate finite-difference models partially circumvents the round-off errors problem, but they soon become computationally intractable if derivatives of high orders are desired.

In Secs. II B and II C, we present a more precise and computationally favourable alternative to the finite difference method to construct an $\mathbf{l}$th derivative of $r_{i\alpha}(\boldsymbol{\xi})$ with respect to $\boldsymbol{\xi}$. Following Eq. (8) we split this task into two parts: differentiation of the Cartesian coordinates $\bar{r}_{i\alpha}(\boldsymbol{\xi})$ of an arbitrary order in the reference, user-defined frame (Sec. II B) and differentiation of the Eckart frame rotation matrix $\mathbf{d}(\boldsymbol{\xi})$ (Sec. II C). Both parts can be applied to any molecule and any choice of the internal coordinates. Then the derivatives of the Cartesian coordinates in the Eckart frame, $r_{i\alpha}(\boldsymbol{\xi})$, in Eq. (8) are evaluated from those of $\mathbf{d}(\boldsymbol{\xi})$ and $\bar{r}_{i\alpha}(\boldsymbol{\xi})$ using the Leibniz product rule as

$$\frac{1}{|\mathbf{l}|!} \left.\frac{\partial^{|\mathbf{l}|} r_{i\alpha}}{\partial\xi_1^{l_1}\dots\partial\xi_M^{l_M}}\right|_{\boldsymbol{\xi}=0} = \sum_{\substack{\mathbf{0}\le\mathbf{k}\le\mathbf{l} \\ \mathbf{k}\in\mathbb{N}^M}} \sum_{\beta=x,y,z} d_{\mathbf{k}}^{(\alpha\beta)} \bar{r}_{\mathbf{l}-\mathbf{k}}^{(i\beta)}, \tag{19}$$

where $\mathbf{l}$ denotes an M-dimensional multi-index defining the order of partial derivative, and $d_{\mathbf{k}}^{(\alpha\beta)}$ and $\bar{r}_{\mathbf{l}-\mathbf{k}}^{(i\beta)}$ are the respective expansion coefficients of $d_{\alpha\beta}(\boldsymbol{\xi})$ and $\bar{r}_{i\beta}(\boldsymbol{\xi})$.

B. "Automatic differentiation" of Cartesian coordinates

Towards constructing the KEO as power series expansions we start from an evaluation of $\mathbf{l}$th-order ($\mathbf{l} \le L$) partial derivatives of Cartesian coordinates in a reference frame $\bar{r}_{i\alpha}(\boldsymbol{\xi})$ with respect to internal coordinates $\boldsymbol{\xi}$, which we intend to do exactly.

Here, we adopt a numerical approach based on the forward accumulation mode AD technique.[78] The basic idea of AD is that every computer program performs series of simple built-in arithmetic operations, such as "+", "∗", "/", etc., and evaluations of simple intrinsic mathematical functions, such as "sin", "cos", "exp", "log", etc., whose single derivatives are well known to arbitrary order. The AD's idea is to couple the differentiation of the single built-ins with derivative accumulation according to the chain rule of differential calculus. The computation of a function in a code fragment is augmented so that the derivatives with respect to the chosen variables are computed along with the value of the function at whichever point the latter is evaluated. The resulting values are exact within the limitations of the floating point arithmetic, but unlike the symbolic differentiation, the result is not a self-contained expression for the derivative that can be used to compute the value of the derivative at arbitrary points.

To illustrate the basic idea of AD we present a small example. Consider the code fragment computing x, y, and z Cartesian components from the input internal coordinates r, α, and τ given by

$$\begin{aligned} x &= r\sin(\alpha)\cos(\tau), \\ y &= r\sin(\alpha)\sin(\tau), \\ z &= r\cos(\alpha). \end{aligned} \tag{20}$$

Assuming the second-order Taylor series expansion of x, y, and z in terms of r, α, and τ, we extend all variables to return the corresponding partial derivatives, along with the values at the reference points r_0, α_0, and τ_0. Thus,

$$x = [x_0, \frac{\partial x}{\partial r}, \frac{\partial x}{\partial \alpha}, \frac{\partial x}{\partial \tau}, \frac{\partial^2 x}{\partial r^2}, \frac{\partial^2 x}{\partial r\partial \alpha}, \frac{\partial^2 x}{\partial r\partial \tau}, \frac{\partial^2 x}{\partial \alpha^2}, \frac{\partial^2 x}{\partial \alpha\partial \tau}, \frac{\partial^2 x}{\partial \tau^2}]$$

$$= [x_0, x_1, x_2, x_3, x_{11}, x_{12}, x_{13}, x_{22}, x_{23}, x_{33}], \tag{21}$$

$$r = [r_0, \frac{\partial r}{\partial r}, \frac{\partial r}{\partial \alpha}, \frac{\partial r}{\partial \tau}, \frac{\partial^2 r}{\partial r^2}, \frac{\partial^2 r}{\partial r\partial \alpha}, \frac{\partial^2 r}{\partial r\partial \tau}, \frac{\partial^2 r}{\partial \alpha^2}, \frac{\partial^2 r}{\partial \alpha\partial \tau}, \frac{\partial^2 r}{\partial \tau^2}]$$

$$= [r_0, r_1, r_2, r_3, r_{11}, r_{12}, r_{13}, r_{22}, r_{23}, r_{33}], \tag{22}$$

and similar expressions for y, z, α, and τ, where subscript "0" indicates that they are taken at reference point. The expansion coefficients of the input variables r, α, and τ become

$$r = [r_0, 1, 0, 0, 0, 0, 0, 0, 0, 0], \tag{23}$$

$$\alpha = [\alpha_0, 0, 1, 0, 0, 0, 0, 0, 0, 0], \tag{24}$$

$$\tau = [\tau_0, 0, 0, 1, 0, 0, 0, 0, 0, 0]. \tag{25}$$

The multiplication operator as well as intrinsic functions "sin" and "cos" in Eq. (20) are also extended to act on the variables being the second-order Taylor polynomials. Invoking the product and the chain rules, we obtain

$$\begin{aligned} a * b = {} & [a_0 b_0, \frac{\partial(ab)}{\partial r}, \frac{\partial(ab)}{\partial \alpha}, \frac{\partial(ab)}{\partial \tau}, \frac{\partial^2(ab)}{\partial r^2}, \frac{\partial^2(ab)}{\partial r\partial \alpha}, \frac{\partial^2(ab)}{\partial r\partial \tau}, \frac{\partial^2(ab)}{\partial \alpha^2}, \frac{\partial^2(ab)}{\partial \alpha\partial \tau}, \frac{\partial^2(ab)}{\partial \tau^2}] \\ = {} & [a_0 b_0, \quad a_1 b_0 + a_0 b_1, \quad a_2 b_0 + a_0 b_2, \quad a_3 b_0 + a_0 b_3, \quad 2a_1 b_1 + a_{11} b_0 + a_0 b_{11}, \quad a_1 b_2 + a_2 b_1 + a_{12} b_0 + a_0 b_{12}, \\ & a_1 b_3 + a_3 b_1 + a_{13} b_0 + a_0 b_{13}, \quad 2a_2 b_2 + a_{22} b_0 + a_0 b_{22}, \quad a_2 b_3 + a_3 b_2 + a_{23} b_0 + a_0 b_{23}, \quad 2a_3 b_3 + a_{33} b_0 + a_0 b_{33}] \end{aligned} \tag{26}$$

and

$$\begin{aligned} \sin(a) = {} & [\sin(a_0), \quad \cos(a_0)a_1, \quad \cos(a_0)a_2, \quad \cos(a_0)a_3, \quad -\sin(a_0)a_1^2 + \cos(a_0)a_{11}, \quad -\sin(a_0)a_1 a_2 + \cos(a_0)a_{12}, \\ & -\sin(a_0)a_1 a_3 + \cos(a_0)a_{13}, \quad -\sin(a_0)a_2^2 + \cos(a_0)a_{22}, \quad -\sin(a_0)a_2 a_3 + \cos(a_0)a_{23}, \quad -\sin(a_0)a_3^2 + \cos(a_0)a_{33}], \end{aligned} \tag{27}$$

where the arrays "a," "b," "$a * b$," and "$\sin(a)$" have the same alignment of the elements as in Eq. (21). The remaining operators and mathematical functions like $\cos(a)$ can be derived with equal ease. Now, if we augment the program code with the above definitions of variables, operators, and intrinsic functions, the derivatives of Eq. (20) will be automatically propagated from derivatives of r, α, τ (Eqs. (23)–(25)) to derivatives of $\cos(\alpha)$, $\sin(\alpha)$, $\cos(\tau)$, and $\sin(\tau)$, then to derivatives of $r\sin(\alpha)$ and $r\cos(\alpha)$, and finally to derivatives of x, y, and z.

We apply this procedure to compute the expansions of Cartesian coordinates in a user-defined reference frame in terms of user-defined internal coordinates. Clearly, our approach is an alternative to the symbolic differentiation. Although in principle by properly choosing the reference frame (e.g., a Z-matrix), the Cartesian coordinates can be analytically expressed in terms of and thus directly differentiated with respect to the internal coordinates symbolically. However, from the standpoint of a general computational approach, this technique has some disadvantages. Most importantly, symbolic derivations must be repeated and converted into a computer code for every new type of molecule and internal coordinates, as well as when higher expansion orders are required. In addition, symbolic expressions, especially for derivatives of high orders and with respect to many variables, may be quite unwieldy resulting in bad performance of the final computer code.

Our Fortran 90 implementation of the forward-mode AD is based on the new derived-type variables with the elements as floating-point coefficients of the finite-order Taylor polynomials. All scalar floating point operations and intrinsic functions are augmented with operations and functions acting on, or having as arguments, the new derived-type variables—the polynomial variables. Each of these operations and intrinsic functions is redefined, through operator overloading, to return not just function values, but a polynomial variable with expansion coefficients calculated according to the chain rules of differential calculus. The latter are generated at a runtime for a given number of variables and polynomial truncation order. We implemented the new derived type together with the functions overloading the standard Fortran operators and intrinsic functions in a separate program module. Using this module to compute the derivatives of a user-defined function demands a few simple modifications in the underlying programming code, namely, one must add a call of AD initializing function and change types of all active variables to the polynomial type. After initialization of the chain rules for a given number of variables and maximal order, the expansion coefficients are automatically propagated starting with the input variables forward to the output variables. To reduce minor round-off errors in AD, we also implemented an option for a 128-bit arithmetic model, supported by some Fortran compilers.

Analytic derivatives of arbitrary orders of all built-in functions and arithmetic operations supported by Fortran 90 language are included into the AD module by construction. More complex operations such as matrix inversion or diagonalisation, that are usually called from the external libraries (e.g., Lapack), cannot be handled automatically by the AD module. However, usually it is not a problem for AD to propagate the derivatives through all arithmetic operations when such complex procedures are included into a numerical definition of a function in question.

C. Expansion of the Eckart frame rotation matrix

To solve the Eckart frame equations, defined by Eq. (9), it is necessary to find a parametrization of an orthogonal frame rotation matrix **d** in terms of three independent parameters such that **d** retains its orthogonality for all possible variations of the parameters. This can be done by several means, the customary one is to use three Euler angles as independent parameters and write **d** in terms of the so-called direction cosine matrix. An alternative quaternion representation of the rotation matrix, which is more numerically convenient and stable compared to Euler angles, has been recently suggested for a solution of the Eckart equations.[62] We follow a different approach and utilize the unconstrained orthogonal parametrization of **d** by writing it in terms of an exponential matrix as

$$\mathbf{d} = e^{-\boldsymbol{\kappa}}, \tag{28}$$

$$\boldsymbol{\kappa}^T = -\boldsymbol{\kappa}, \tag{29}$$

where the elements of a skew-symmetric 3×3 matrix $\boldsymbol{\kappa}$ are real and the minus sign in the exponential is conventional. In this representation, the orthogonality condition is automatically fulfilled at any values of three independent elements κ_{xy}, κ_{xz}, and κ_{yz}, which now play the role of unknowns that are to be determined from solution of the Eckart equations,

$$\mathbf{u}e^{\boldsymbol{\kappa}} - e^{-\boldsymbol{\kappa}}\mathbf{u}^T = 0, \tag{30}$$

where **u** is defined in Eq. (10). A simple rearrangement of terms in Eq. (30) provides a more convenient form of this expression, given by

$$\mathbf{u}\boldsymbol{\kappa} + \boldsymbol{\kappa}\mathbf{u}^T = \boldsymbol{\lambda}\mathbf{u}^T - \mathbf{u}\boldsymbol{\lambda}^T, \tag{31}$$

where

$$\boldsymbol{\lambda} = e^{-\boldsymbol{\kappa}} + \boldsymbol{\kappa} = \mathbf{I} + \frac{1}{2}\boldsymbol{\kappa}\cdot\boldsymbol{\kappa} - \frac{1}{6}\boldsymbol{\kappa}\cdot\boldsymbol{\kappa}\cdot\boldsymbol{\kappa} + \cdots, \tag{32}$$

that leads to a simple iterative approach for determining the elements of $\boldsymbol{\kappa}$. Equation (31) can be recast in a form more convenient for numerical solution as given by

$$\begin{pmatrix} u_{xx}+u_{yy} & u_{yz} & -u_{xz} \\ u_{zy} & u_{xx}+u_{zz} & u_{xy} \\ -u_{zx} & u_{yx} & u_{yy}+u_{zz} \end{pmatrix} \begin{pmatrix} \kappa_{xy} \\ \kappa_{xz} \\ \kappa_{yz} \end{pmatrix} = \sum_{\alpha=x,y,z} \begin{pmatrix} \lambda_{x\alpha}u_{y\alpha} - \lambda_{y\alpha}u_{x\alpha} \\ \lambda_{x\alpha}u_{z\alpha} - \lambda_{z\alpha}u_{x\alpha} \\ \lambda_{y\alpha}u_{z\alpha} - \lambda_{z\alpha}u_{y\alpha} \end{pmatrix}. \tag{33}$$

A simple starting approximation for $\boldsymbol{\lambda}$ is obtained by setting $\boldsymbol{\kappa} = 0$, which is then inserted into the right-hand side of Eq. (33) and subsequently used to obtain a new estimate for $\boldsymbol{\kappa}$ by solving the system of linear equations. The matrix on the left-hand side is common for all iterations and, thus, its inverse is computed only once. The iterative process is continued until convergence is reached. The number of iterations will depend on the magnitude of elements of the $\boldsymbol{\kappa}$ matrix, in other words on how "far" the reference frame is angularly displaced from the Eckart frame. From our experience for various four- to six-atomic molecules and various definitions of reference frames, the convergence of 10^{-30} for $\boldsymbol{\kappa}$ is reached within ten iterations.

An iterative solution of Eq. (31) as defined by Eqs. (32) and (33) requires an evaluation of the exponential of a skew-symmetric matrix at each iteration. This can be computed either by expanding the exponential in a Taylor series, or using the explicit Rodrigues formula (see, for instance, Ref. 81), or the spectral decomposition. The computational merit of various methods will depend on the magnitude of the matrix argument. The Taylor series approach is the most straightforward, however, for quick convergence (in a small number of expansion terms), it requires the argument to be close to the null matrix. When this is not the case, the computation can still be efficiently done by employing the scaling and squaring technique,[82] which exploits the fundamental and unique property of the exponential function,

$$e^{-\boldsymbol{\kappa}} = e^{-\boldsymbol{\kappa}/2}e^{-\boldsymbol{\kappa}/2}. \tag{34}$$

Using this property, $e^{-\boldsymbol{\kappa}}$ can be calculated recursively from $e^{-\boldsymbol{\kappa}/2^N}$ by a repeated N-times squaring, where the latter can be evaluated accurately and efficiently by a Taylor series expansion. Depending on the magnitude of the elements of $\boldsymbol{\kappa}$, N can be chosen such that the norm of $\boldsymbol{\kappa}/2^N$ becomes sufficiently small.

The proposed iterative approach for constructing the Eckart frame rotation matrix can be naturally adapted as a power series representation. Indeed, since the rotation matrix is a continuous function of internal coordinates, the expansion coefficients can be obtained by simple differentiation of Eq. (9)

with respect to the internal coordinates, where we can employ the AD approach. In fact, this approach could be directly applied to differentiate any function appearing in Eq. (33). Nonetheless, in the following we optimize the differential calculus specifically for the Eckart equations towards an efficient and stable numerical method to compute the power series expansion of the corresponding solution.

Applying the generalized Leibniz rule, we obtain

$$\mathbf{u}_0\mathbf{d}_{\mathbf{l}}^T - \mathbf{d}_{\mathbf{l}}\mathbf{u}_{\mathbf{0}}^T = \sum_{\substack{\mathbf{0}\le\mathbf{k}<\mathbf{l}\\ \mathbf{k}\in\mathbb{N}^M}} \left(\mathbf{d}_{\mathbf{k}}\mathbf{u}_{\mathbf{l}-\mathbf{k}}^T - \mathbf{u}_{\mathbf{k}}\mathbf{d}_{\mathbf{l}-\mathbf{k}}^T\right), \qquad (35)$$

where $\mathbf{l} = \{l_1,\dots,l_M\}$ is an M-dimensional multi-index defining the order of partial differentiation and $\mathbf{d}_{\mathbf{l}}$ and $\mathbf{u}_{\mathbf{l}}$ denote the respective expansion coefficients for $\mathbf{d}$ and $\mathbf{u}$ (the latter is given by Eq. (10)). Likewise to the expression for expansion coefficients of the $\mathbf{s}$-matrix, defined in Eq. (16), Eq. (35) suggests a recursive procedure to generate expansion coefficients of the $\mathbf{d}$-matrix starting from the coefficients of $\mathbf{l} = \mathbf{0}$ upwards to higher orders. Equation (35) can be also given in a linear system form of Eq. (33) by replacing $\boldsymbol{\kappa}$ and $\boldsymbol{\lambda}$ with $\boldsymbol{\kappa}_{\mathbf{l}}$ and $\boldsymbol{\lambda}_{\mathbf{l}}$, respectively, and augmenting the right-hand side vector with the right-hand side of Eq. (35). For each expansion coefficient $\boldsymbol{\kappa}_{\mathbf{l}}$, the resulting system of nonlinear equations is solved iteratively starting from $\boldsymbol{\lambda}_{\mathbf{l}} = 0$. At each iteration, a new estimate for $\boldsymbol{\kappa}_{\mathbf{l}}$ is obtained by solving a system of linear equations where $\boldsymbol{\lambda}_{\mathbf{l}}$ is updated in accord with Eq. (32) as $\boldsymbol{\lambda}_{\mathbf{l}} = e_{\mathbf{l}}^{-\boldsymbol{\kappa}} + \boldsymbol{\kappa}_{\mathbf{l}}$. The expansion coefficients of the exponential $e_{\mathbf{l}}^{-\boldsymbol{\kappa}}$ can be evaluated by employing the Taylor series expansion technique combined with the product rule as

$$e_{\mathbf{l}}^{-\boldsymbol{\kappa}} = \sum_{i>0}(-1)^i\boldsymbol{\kappa}_{\mathbf{l}}^{(i)}, \qquad (36)$$

$$\boldsymbol{\kappa}_{\mathbf{l}}^{(1)} = \boldsymbol{\kappa}_{\mathbf{l}}, \qquad (37)$$

$$\boldsymbol{\kappa}_{\mathbf{l}}^{(i)} = [\boldsymbol{\kappa}\boldsymbol{\kappa}^{(i-1)}]_{\mathbf{l}} = \sum_{\substack{\mathbf{0}\le\mathbf{k}\le\mathbf{l}\\ \mathbf{k}\in\mathbb{N}^M}} \boldsymbol{\kappa}_{\mathbf{k}}\boldsymbol{\kappa}_{\mathbf{l}-\mathbf{k}}^{(i-1)}, \qquad (38)$$

where $\boldsymbol{\kappa}_{\mathbf{l}}$ represent values of the target expansion coefficients at the current iteration, assuming that all lower-order expansion coefficients of $\boldsymbol{\kappa}$ and of its power $\boldsymbol{\kappa}^{(i)}$ have been already calculated in the previous steps of the recursive procedure. To accelerate the convergence of the Taylor series expansion and thus reduce the number of power functions $\boldsymbol{\kappa}^{(i)}$, the scaling method defined by Eq. (34) can be employed. It remains only to define the expansion coefficients $\mathbf{u}_{\mathbf{l}}$, which can be easily evaluated using Eq. (10) as

$$u_{\mathbf{l}}^{(\alpha\beta)} = \sum_i^N m_i r_{i\alpha}^{(\mathrm{eq})}\bar{r}_{\mathbf{l}}^{(i\beta)}, \qquad (39)$$

where $\bar{r}_{\mathbf{l}}^{(i\beta)}$ denote the expansion coefficients of the reference-frame Cartesian coordinates calculated prior to solving the Eckart frame equations using the technique outlined in Sec. II B.

In our derivations, no assumptions have been made on the orientation of the equilibrium coordinate system $r_{i\alpha}^{(\mathrm{eq})}$ in Eqs. (10) and (39). It can be chosen to coincide with the reference frame $\bar{r}_{i\alpha}(\boldsymbol{\xi})$ (e.g., Z-matrix) at equilibrium values of internal coordinates, i.e., $r_{i\alpha}^{(\mathrm{eq})} = \bar{r}_{i\alpha}(\boldsymbol{\xi}^{(\mathrm{eq})})$, or the PAS frame (Eq. (11)). The former choice greatly simplifies the iterative Eckart solution of Eq. (35) by reducing it to a system of linear equations. Indeed, in this case the corresponding rotation matrix $\mathbf{d}$ at equilibrium becomes the identity matrix and its derivatives are simply given by the derivatives of $\boldsymbol{\kappa}$. The expansion coefficients $\mathbf{d}_{\mathbf{l}}$ in Eq. (35) are then obtained by repeatedly solving the following system of linear equations:

$$\mathbf{u}_0\boldsymbol{\kappa}_{\mathbf{l}} + \boldsymbol{\kappa}_{\mathbf{l}}\mathbf{u}_{\mathbf{0}}^T = \sum_{\substack{\mathbf{0}\le\mathbf{k}<\mathbf{l}\\ \mathbf{k}\in\mathbb{N}^M}} \left(-\mathbf{u}_{\mathbf{k}}\boldsymbol{\kappa}_{\mathbf{l}-\mathbf{k}} - \boldsymbol{\kappa}_{\mathbf{k}}\mathbf{u}_{\mathbf{l}-\mathbf{k}}^T\right), \qquad (40)$$

for each expansion coefficient $\boldsymbol{\kappa}_{\mathbf{l}}$ utilizing the coefficients of the lower orders obtained at previous iterations. Using the PAS frame for the equilibrium configuration has an advantage of optimal decoupling in the pure rotational part of the KEO, although it demands the non-linear solution of the Eckart equations (unless the reference frame ≡ PAS). As confirmed by our multiple studies for medium size molecules, the computational merit of minimizing the pure rotational couplings of the KEO is insignificant in variational calculations where all ro-vibrational interactions are taken into account, albeit may be useful for certain approximate perturbation theory models.

In principle, there exist eight solutions of the Eckart frame equations corresponding to eight possible variations of the plus and minus signs at the absolute values of elements of the skew-symmetric matrix $\boldsymbol{\kappa}$, defined in Eq. (28), see also Ref. 61. In our method, all derivatives are obtained recursively starting from the zero-order solution, therefore our selection (one out of eight Eckart solutions) is uniquely defined by the initial choice of the signs in the zero-order matrix $\boldsymbol{\kappa}$. It should also be noted that the direct numerical methods for the Eckart equations of Dymarsky and Kudin[61] and Krasnoshchekov *et al.*[62] can also be adapted to the AD technique developed here. The essential part of both methods is the solution of an eigenvalue problem (3×3 and 4×4, respectively), which can be cast into a form similar to Eqs. (31) and (32) using the exponential ansatz for the frame rotation matrix. In fact, a very similar approach is already used in our implementation of the PAS embedding as a part of the diagonalisation of 3×3 inertia matrix, see Eq. (11).

III. EXPANSION OF POTENTIAL AND DIPOLE MOMENT FUNCTIONS

The PES and dipole moment surface (DMS) are "external" functions that are usually obtained from electronic structure calculations, and are sometimes also refined against the experimental data. Our variational approach requires that both the KEO and PES are represented as power series in terms of the same internal coordinates ξ_i (or simple one dimensional functions $f_i(\xi_i)$, e.g., Morse and cosine).[3] This also holds for all properties to be evaluated, for example, electric dipole moment,[83] polarizability,[84] and spin-spin couplings.[85] In principle, these functions may be prepared in this way, otherwise, as a general case, the AD technique described above is employed to expand the PES and, for example, DMS in terms of $\xi_1,\dots,\xi_{3N-6}$ internal coordinates providing that the analytic transformation between representations is implemented. Following Eq. (13), the potential energy and dipole moment functions can be written as

$$V(\boldsymbol{\xi}) = \sum_{0 \le |\mathbf{l}| \le L_V} f_{\mathbf{l}} \xi_1^{l_1} \dots \xi_M^{l_M}, \tag{41}$$

$$\mu_\alpha(\boldsymbol{\xi}) = \sum_{0 \le |\mathbf{l}| \le L_\mu} \mu_{\mathbf{l}}^{(\alpha)} \xi_1^{l_1} \dots \xi_M^{l_M} \quad (\alpha = x, y, z), \tag{42}$$

where $\mathbf{l} = \{l_1, \dots, l_M\}$ denotes an expansion multi-index, $f_{\mathbf{l}}$ and $\mu_{\mathbf{l}}^{(\alpha)}$ are the respective expansion coefficients of the PES and a Cartesian α-component of the DMS, and L_V and L_μ are the respective maximal expansion orders. In this manner, at least in principle, any arbitrary analytical PES and DMS available in the literature are automatically re-expanded and directly employed in our variational calculations. It should be noted, however, that in some special cases of complicated functional forms the re-expansion may lead to slow or lack of convergence and thus has to be checked.

Properties represented by vectors or tensors such as dipole moment $\boldsymbol{\mu}$ require an additional transformation from the original, user-defined, frame to the body-fixed Cartesian frame used in the variational calculations, e.g., Eckart frame. In this case the re-expansion is divided into the following steps. First, the three dipole moment components μ_α defined in the original frame are re-expanded in terms of the internal coordinates $\xi_1, \dots, \xi_{3N-6}$, if different from the original, using the AD tool. Second, the expansion of the transformation matrix between the original and the Eckart frames is computed. Towards this, we designed an AD-specific function that returns elements of the transformation matrix in terms of the Cartesian coordinates of each atom in the Eckart frame. The latter are precomputed and stored using the methods described above at the stage of the KEO construction, and converted into the AD-specific variables (see Sec. II B). Depending on the type of the original frame used, an inverse of the transformation matrix may be required. In this case the expansion is obtained using a

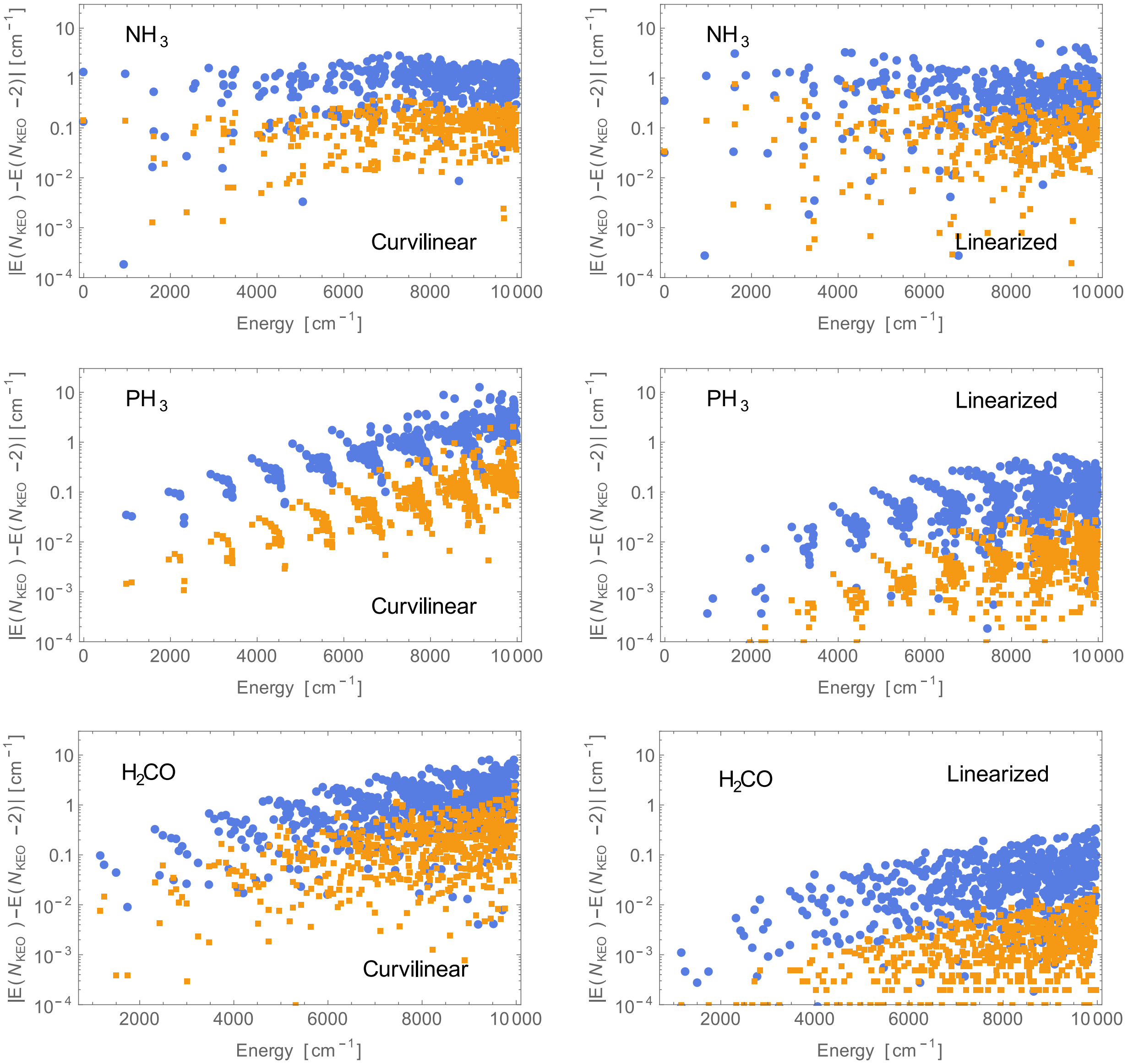

FIG. 1. Convergence of the KEO power series expansion for vibrational energies of NH$_3$, PH$_3$, and H$_2$CO employing curvilinear and linearized internal coordinate models. The absolute values for energy differences $|E(N_{\rm KEO}) - E(N_{\rm KEO} - 2)|$ are drawn for series truncation orders $N_{\rm KEO} = 6$ and 8 in blue circles and orange squares, respectively.

recursive procedure similar to Eq. (16), where **t** and **s** are replaced by the transformation matrix and its inverse, respectively. The final expansion of the DMS is obtained as a product of two polynomials obtained at steps 1 and 2. The transformation of different tensorial properties and/or to different molecular frames can be performed in a similar manner.

IV. SUMMARY OF COMPUTATIONAL PROCEDURE

In the following, we summarize the procedure for the numerical construction of the power series expansion of the Hamiltonian using the AD technique as it is implemented in TROVE.[3]

Before starting any calculations, a user must provide a Fortran 90 function that returns the Cartesian coordinates $\bar{r}_{i\alpha}(\boldsymbol{\xi})$ $(\alpha = x, y, z)$ of each atom i in the chosen reference frame for a given set of the internal coordinates ξ_k $(k = 1, \dots, 3N-6)$, unless it is already available in TROVE for a given molecular structure or one of the general (e.g., Z-matrix) transformations is used. The expansion of the Hamiltonian is summarized as follows.

1. Choose the reference frame and type of embedding (e.g., Eckart frame) for the body-fixed frame used for the KEO, and the internal coordinates $\boldsymbol{\xi}$ (e.g., as displacements of bond lengths, valence bond or dihedral angles).
2. Compute the expansion of the Cartesian coordinates in terms of the internal coordinates invoking either a user-provided subroutine or using one of the general transformations available in TROVE (e.g., Z-matrix). The subroutine must be compatible with the AD library, which usually requires only a small modification of the standard Fortran data types to the AD-specific types (Sec. II B). The maximal order of differentiation P is determined by the maximal requested expansion order for the kinetic energy matrix Q and pseudopotential R, as $P = \max(Q+1, P+3)$ (see Eqs. (2) and (3)). After initialization of the chain rule expressions for a given P and number of internal coordinates, all required expansion coefficients are computed as derivatives via AD.
3. Compute the expansion of the Eckart frame rotation matrix using the expansion coefficients of the reference-frame Cartesian coordinates obtained at the previous step. This requires a recursive solution of the system of non-linear equations, given by Eqs. (31)–(35), which may become a linear system for some reference frames as defined in Eq. (40).
4. Compute derivatives of the Cartesian coordinates in the Eckart frame. Using Eq. (19), all derivatives are obtained from the expansion coefficients of the reference-frame Cartesian coordinates and the Eckart-frame rotation matrix.
5. Construct expansions of the **t** matrix in accordance with Eqs. (17) and (18) and apply Eq. (16) to convert it into expansions of the **s** matrix.
6. Construct expansions of the kinetic energy matrix $G_{\lambda\mu}$ and pseudopotential U from the expansion coefficients of the **s** matrix using relations in Eq. (15).

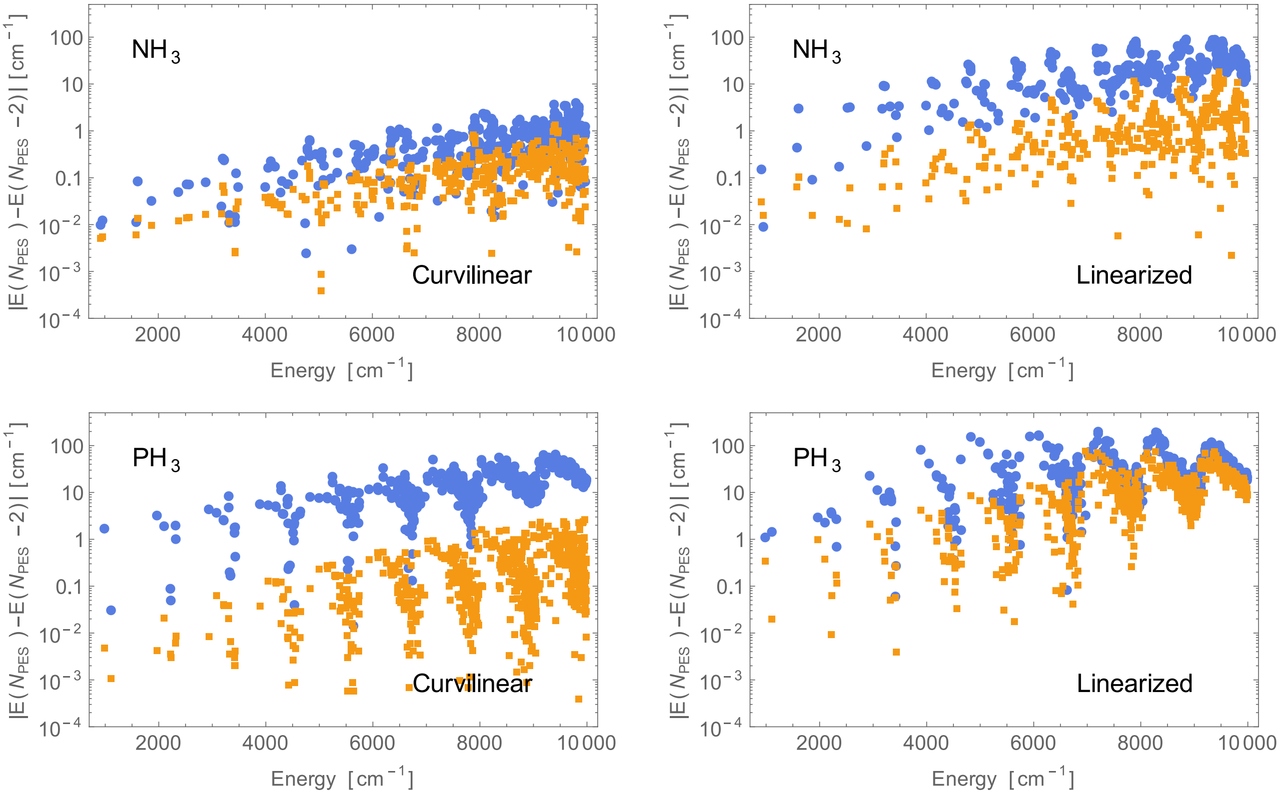

FIG. 2. Convergence of the PES power series expansion for vibrational energies of NH_3 and PH_3 employing curvilinear and linearized internal coordinate models. The absolute values for energy differences $|E(N_{PES}) - E(N_{PES}-2)|$ are drawn for series truncation orders $N_{PES} = 6$ and 8 in blue circles and orange squares, respectively.

7. Construct an expansion of the potential energy function in terms of the internal coordinates by means of AD. In principle, the PES may be provided by the user directly in the form intended for variational calculations. In this case, the corresponding AD calls are skipped.
8. Construct expansions of the dipole moment components (or any other molecular property tensor) in terms of the internal coordinates by means of AD first in the reference frame and then transform them into the Eckart frame by means of the transformation matrix obtained at step 2 of procedure

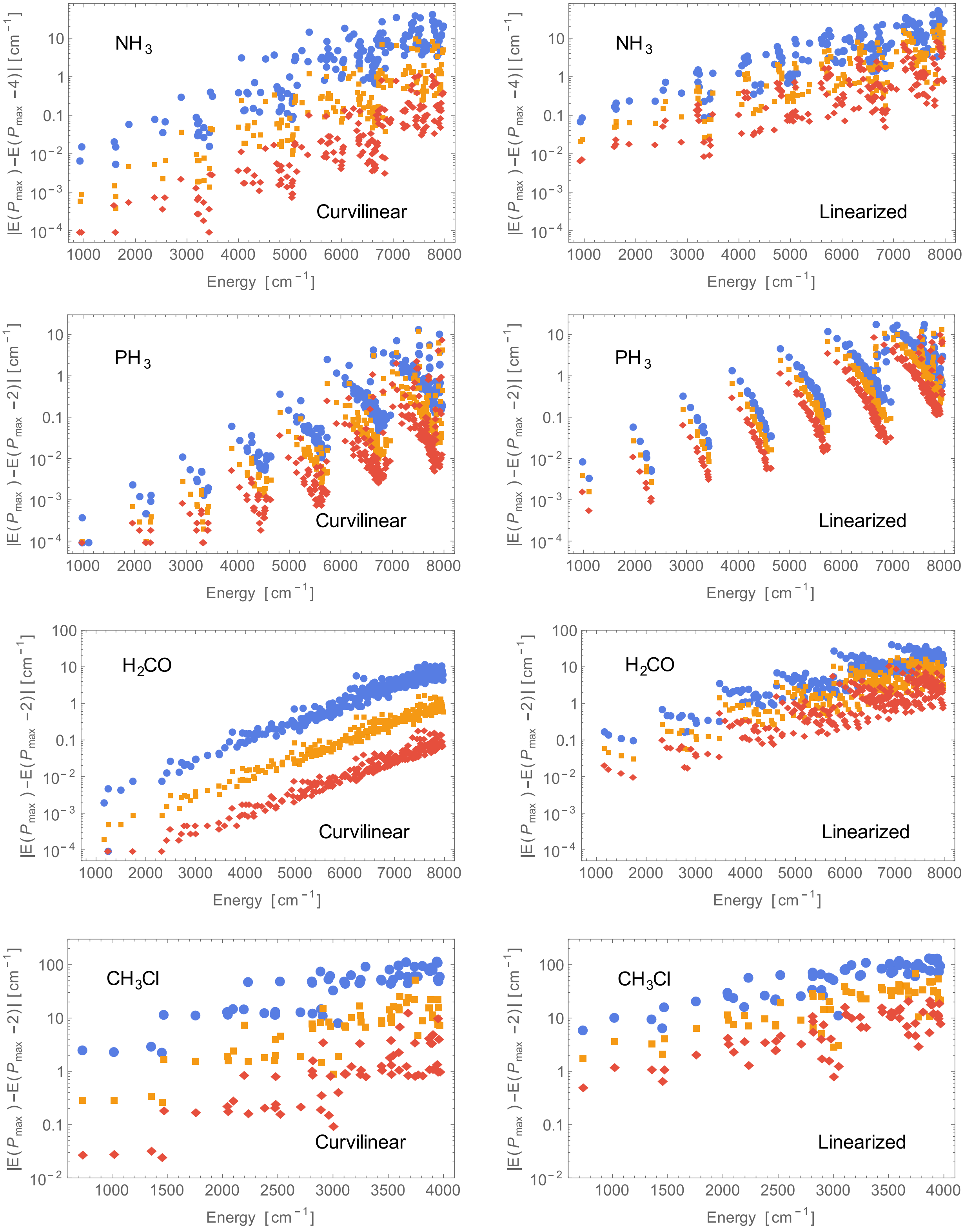

FIG. 3. Basis set convergence for vibrational energies of NH_3, PH_3, H_2CO, and CH_3Cl employing curvilinear and linearized internal coordinate models. The absolute energy differences $|E(P_{\max})-E(P_{\max}-4)|$ for NH_3 and $|E(P_{\max})-E(P_{\max}-2)|$ for other molecules are drawn for three basis sets truncated at increasing polyad numbers $P_{\max}=P_1$, P_2, and P_3 in blue circles, orange squares, and red diamonds, respectively, where $\{P_1,P_2,P_3\}=\{24,28,32\}$ for NH_3, $\{16,18,20\}$ for PH_3, $\{12,14,16\}$ for H_2CO, and $\{8,10,12\}$ for CH_3Cl.

TABLE I. Errors (in cm^{-1}) in the vibrational energy levels of NH_3 calculated employing curvilinear (Curv) and linearized (Lin) internal coordinate models. The energies are listed relative to the zero-point energy (0^+) of 7436.82 cm^{-1}. The reference energies are taken from Mátyus *et al.*[5] (Mátyus) where they were obtained using the exact KEO approach and converged to within 0.05 cm^{-1}; the quantum numbers are as defined in Derzi *et al.*[97]

Assig	Sym	Mátyus	Curv	Lin
0^+	A_1'	0.00	0.00	0.00
0^-	A_2''	0.79	0.00	0.01
ν_2^+	A_1'	932.41	0.00	−0.01
ν_2^-	A_2''	968.15	0.00	−0.01
$2\nu_2^+$	A_1'	1597.26	0.00	−0.01
ν_4^+	E'	1625.62	−0.04	−0.68
ν_4^-	E''	1626.73	−0.04	−0.33
$2\nu_2^-$	A_2''	1882.18	0.00	−0.08
$3\nu_2^+$	A_1'	2384.20	0.00	0.00
$(\nu_2+\nu_4)^+$	E'	2539.61	−0.01	−0.33
$(\nu_2+\nu_4)^-$	E''	2585.39	−0.04	−0.41
$3\nu_2^-$	A_2''	2895.74	0.00	−0.08
$2\nu_2+\nu_4$	E'	3189.11	−0.01	−0.39
$2\nu_4^{0,+}$	A_1'	3214.47	0.00	−0.02
$2\nu_4^{0,-}$	A_2''	3216.15	0.00	−0.02
$2\nu_4^{2,+}$	E'	3238.55	−0.02	0.07
$2\nu_4^{2,-}$	E''	3240.05	−0.03	0.05
ν_1^+	A_1'	3335.78	0.00	−0.02
ν_1^-	A_2''	3336.84	0.01	−0.43
ν_3^+	E'	3443.92	−0.01	−0.03
ν_3^-	E''	3444.27	−0.01	0.03
$4\nu_2^+$	A_1'	3463.00	0.00	−0.02
$(2\nu_2+\nu_4)^-$	E''	3502.44	−0.01	0.02
$(3\nu_2+\nu_4)^+$	E'	4008.04	−0.01	−0.02
$4\nu_2^+$	A_2''	4062.47	0.01	−0.29
$(\nu_2+2\nu_4^0)^+$	A_1'	4112.42	0.00	−0.01
$(\nu_2+2\nu_4^2)^+$	E'	4133.22	−0.01	−0.05
$(\nu_2+2\nu_4^0)^-$	A_2''	4171.08	0.02	−0.36
$(\nu_2+2\nu_4^2)^-$	E''	4191.09	−0.02	−0.04
$(\nu_1+\nu_2)^+$	A_1'	4294.13	0.01	−0.01
$(\nu_1+\nu_2)^-$	A_2''	4319.77	0.01	−0.24
$(\nu_2+\nu_3)^+$	E'	4416.94	0.00	0.01
$(\nu_2+\nu_3)^-$	E''	4435.58	0.01	−0.56
$(3\nu_2+\nu_4)^-$	E''	4531.32	0.00	−0.07
$5\nu_2^+$	A_1'	4695.92	0.01	−0.06
$(2\nu_2+2\nu_4^0)^+$	A_1'	4753.71	0.01	−0.06
$(2\nu_2+2\nu_4^2)^+$	E'	4772.19	0.02	−0.39
$3\nu_4^{1,+}$	E'	4796.02	0.00	−0.06
$3\nu_4^{1,-}$	E''	4798.30	−0.01	−0.02
$3\nu_4^{3,+}$	A_1'	4838.67	0.00	−0.01
$3\nu_4^{3,+}$	A_2'	4838.83	0.00	0.01
$3\nu_4^{3,-}$	A_2''	4840.64	0.00	0.01
$3\nu_4^{3,-}$	A_1''	4840.88	0.00	−0.14
$(\nu_3+\nu_4)^+$	E'	4954.10	−0.01	−0.05
$(\nu_3+\nu_4)^-$	E''	4955.35	−0.01	−0.01
$(\nu_1+2\nu_2)^+$	A_1'	4999.21	−0.01	−0.13
$(\nu_1+\nu_4)^+$	A_2'	5049.17	0.00	−0.02
$(\nu_1+\nu_4)^-$	A_1''	5049.82	−0.02	−0.20
$(\nu_3+\nu_4)^{2,+}$	E'	5051.78	0.00	−0.55
$(\nu_3+\nu_4)^{2,-}$	E''	5052.37	0.01	−0.39
$(\nu_3+\nu_4)^{0,-}$	A_2''	5065.64	0.00	−0.01
$(\nu_3+\nu_4)^{0,+}$	A_1'	5065.65	−0.01	−0.08
$(2\nu_2+2\nu_4^0)^-$	A_2''	5092.98	0.01	−0.09
$(4\nu_2+\nu_4)^+$	E'	5106.21	0.03	−1.65
$(2\nu_2+2\nu_4^2)^-$	E''	5112.82	−0.01	−0.24
$(\nu_1+2\nu_2)^+$	E'	5143.77	0.01	−0.99
$(\nu_1+2\nu_2)^-$	A_2''	5232.82	0.00	−0.02
$(2\nu_2+\nu_3)^-$	E''	5352.86	0.01	−0.90
$5\nu_2^-$	A_2''	5362.51	0.02	−0.68
$(3\nu_2+2\nu_4^0)^+$	A_1'	5603.91	−0.01	−0.13
$(3\nu_2+2\nu_4^2)^+$	E'	5623.30	0.00	−0.02
$(\nu_2+3\nu_4^1)^+$	E'	5672.94	0.01	−1.46
$(4\nu_2+\nu_4)^-$	E''	5709.42	−0.01	−0.99
$(\nu_2+3\nu_4^3)^+$	A_1'	5712.38	−0.01	0.03
$(\nu_2+3\nu_4^3)^+$	A_2'	5713.59	0.02	−0.47
$(3\nu_2+\nu_1)^+$	A_1'	5736.53	−0.01	0.03
$(\nu_2+3\nu_4^1)^-$	E''	5750.80	0.01	−0.95
$(\nu_2+3\nu_4^3)^-$	A_2''	5784.87	−0.05	−0.56
$(\nu_2+3\nu_4^3)^-$	A_1''	5785.52	0.00	0.01
$(3\nu_2+\nu_3)^+$	E'	5855.64	0.00	−0.05

described in Sec. III. The expansion of the DMS in the reference frame may be provided by the user.

After expansions of all operators are constructed, they enter the general variational procedure of TROVE described in detail in Refs. 3 and 86.

V. MOLECULAR INVESTIGATIONS

We presented here a general and numerically quite intensive procedure to construct a power series expansion of the ro-vibrational Hamiltonian, essentially aiming at exploiting the curvilinear coordinates while at the same time using the Eckart frame. Now, it is worthwhile examining what are the potential advantages of using the curvilinear coordinates for expansion of the ro-vibrational Hamiltonian instead of more simple linearized or normal coordinates. There are two aspects we want to benefit from by picking one or other coordinate system: first, the convergence of the power series expansions of the KEO and PES towards the exact limits, and second, the convergence of the eigen-solution towards the complete basis set limit. The latter is the most important aspect as the computational expenses of variational calculations scale nearly exponentially with respect to the basis set size. We selected a set of test molecules, NH_3, PH_3, H_2CO, and CH_3Cl, with their respective PESs taken from Refs. 87–90. These molecules are the subject of extensive computational studies[13,14,88,91,92] as part of the ExoMol project.[93] The curvilinear and linearized internal coordinates along with the basis set polyad structures for these molecules are defined, following the same setup as in Refs. 87, 88, 90, and 94. In all nuclear-motion calculations we used the atomic masses (in a.m.u.) $m_{\mathrm{H}} = 1.007\,825\,05$, $m_{\mathrm{N}} = 14.003\,074$, $m_{\mathrm{O}} = 15.994\,914\,63$, $m_{\mathrm{P}} = 30.973\,762$, and $m_{\mathrm{Cl}} = 34.968\,852\,721$. One may note that for H_2CO and NH_3 we use outdated PESs, even though more accurate versions are available in the literature. The reason is that only for these PESs very accurate independent nuclear-motion predictions for large number of vibrational states are available,[5,9] which is useful for verification of our results. For all molecules, in

TABLE II. Errors (in cm^{-1}) in the vibrational energy levels of H_2CO calculated employing curvilinear (Curv) and linearized (Lin) internal coordinate models. The reference energies are taken from Avila and Carrington[9] (Avila) where they were obtained using the exact KEO approach and converged to within 0.005 cm^{-1}.

Assig	Sym	Avila	Curv	Lin
ZPVE	A_1	5777.45	0.00	0.00
ν_4	B_1	1171.09	0.00	−0.02
ν_6	B_2	1252.89	0.00	0.00
ν_3	A_1	1508.60	0.00	0.01
ν_2	A_1	1749.66	0.00	−0.01
$2\nu_4$	A_1	2332.72	0.00	−0.14
$\nu_4+\nu_6$	A_2	2431.05	0.01	−0.03
$2\nu_6$	A_1	2501.93	0.02	0.00
$\nu_3+\nu_4$	B_1	2679.48	0.00	−0.02
$\nu_3+\nu_6$	B_2	2728.98	0.02	−0.07
ν_1	A_1	2782.83	0.01	0.05
ν_5	B_2	2841.66	0.01	0.08
$\nu_2+\nu_4$	B_1	2913.26	0.00	−0.05
$\nu_2+\nu_6$	B_2	3006.72	0.01	0.03
$2\nu_3$	A_1	3015.72	0.01	0.04
$\nu_2+\nu_3$	A_1	3250.40	0.00	0.00
$2\nu_2$	A_1	3479.87	0.00	−0.02
$3\nu_4$	B_1	3485.00	0.00	−0.70
$2\nu_4+\nu_6$	B_2	3596.67	0.00	−0.29
$\nu_4+2\nu_6$	B_1	3688.91	0.03	−0.11
$3\nu_6$	B_2	3747.46	0.06	−0.04
$\nu_3+2\nu_4$	A_1	3840.19	−0.01	−0.29
$\nu_3+\nu_4+\nu_6$	A_2	3902.60	0.02	−0.25
$\nu_1+\nu_4$	B_1	3946.76	0.01	0.11
$\nu_3+2\nu_6$	A_1	3948.76	0.06	−0.11
$\nu_4+\nu_5$	A_2	4001.16	0.01	0.11
$\nu_1+\nu_6$	B_2	4027.21	0.02	0.12
$\nu_2+2\nu_4$	A_1	4066.64	0.00	−0.35
$\nu_5+\nu_6$	A_1	4088.50	0.02	0.13
$\nu_2+\nu_4+\nu_6$	A_2	4175.54	0.00	−0.07
$2\nu_3+\nu_4$	B_1	4186.18	0.00	−0.03
$2\nu_3+\nu_6$	B_2	4210.65	0.04	−0.07
$\nu_2+2\nu_6$	A_1	4257.92	0.02	0.04
$\nu_1+\nu_3$	A_1	4265.91	0.01	0.06
$\nu_3+\nu_5$	B_2	4345.07	0.01	0.18
$\nu_2+\nu_3+\nu_4$	B_1	4413.59	0.00	−0.10
$\nu_2+\nu_3+\nu_6$	B_2	4479.95	0.02	−0.06
$3\nu_3$	A_1	4520.33	0.01	0.08
$\nu_1+\nu_2$	A_1	4533.06	0.01	0.01
$\nu_2+\nu_5$	B_2	4573.56	0.01	0.03
$4\nu_4$	A_1	4627.89	−0.01	−1.95
$2\nu_2+\nu_4$	B_1	4635.88	0.00	−0.15
$2\nu_2+\nu_6$	B_2	4744.11	0.01	0.03
$\nu_2+2\nu_3$	A_1	4749.26	0.00	0.01
$3\nu_4+\nu_6$	A_2	4751.76	−0.02	−0.98
$2\nu_4+2\nu_6$	A_1	4858.07	−0.01	−0.47
$\nu_4+3\nu_6$	A_2	4945.24	0.08	−0.17
$2\nu_2+\nu_3$	A_1	4972.27	0.01	−0.04
$4\nu_6$	A_1	4990.18	0.15	−0.02
$\nu_3+3\nu_4$	B_1	4991.38	−0.02	−1.10
$\nu_3+2\nu_4+\nu_6$	B_2	5060.41	0.01	−0.75
$\nu_1+2\nu_4$	A_1	5100.24	0.01	−0.09
$\nu_3+\nu_4+2\nu_6$	B_1	5129.86	0.09	−0.30
$2\nu_4+\nu_5$	B_2	5150.71	0.00	−0.09
$\nu_3+3\nu_6$	B_2	5168.17	0.15	0.01
$3\nu_2$	A_1	5191.38	0.04	−0.03
$\nu_1+\nu_4+\nu_6$	A_2	5197.58	0.01	0.11
$\nu_2+3\nu_4$	B_1	5211.64	−0.01	−1.35
$\nu_4+\nu_5+\nu_6$	B_1	5258.97	0.02	0.07
$\nu_1+2\nu_6$	A_1	5265.13	0.04	−0.09
$\nu_5+2\nu_6$	B_2	5324.79	0.03	−0.21
$\nu_2+2\nu_4+\nu_6$	B_2	5336.89	0.01	−0.31
$2\nu_3+2\nu_4$	A_1	5345.47	−0.02	−0.36
$2\nu_3+\nu_4+\nu_6$	A_2	5382.60	0.05	−0.22
$2\nu_3+2\nu_6$	A_1	5403.95	0.12	0.01
$\nu_1+\nu_3+\nu_4$	B_1	5430.39	0.01	0.12
$\nu_2+\nu_4+2\nu_6$	B_1	5434.23	0.02	−0.16
$\nu_1+\nu_3+\nu_6$	B_2	5442.23	0.10	−0.47
$2\nu_1$	A_1	5471.90	0.16	0.31
$\nu_2+3\nu_6$	B_2	5504.07	0.06	0.01
$\nu_3+\nu_4+\nu_5$	A_2	5506.72	0.00	0.16
$\nu_1+\nu_5$	B_2	5542.29	0.08	0.64
$\nu_3+\nu_5+\nu_6$	A_1	5557.36	0.05	−0.13
$\nu_2+\nu_3+2\nu_4$	A_1	5567.82	−0.01	−0.52
$\nu_2+\nu_3+\nu_4+\nu_6$	A_2	5644.80	0.01	−0.35
$2\nu_5$	A_1	5653.40	0.04	0.29

the expansions of PESs we employed Morse type variables for stretching vibrational coordinates, curvilinear and linearized. For NH_3, the expansion of the ro-vibrational Hamiltonian was built around the non-rigid reference configuration,[95] which was defined for the umbrella-motion vibrational coordinate on a grid of 4000 points with displacements covering potential energies up to 40 000 cm^{-1} above the minimum. To control the size of the vibrational basis set we used the polyad number P, which is not allowed to exceed the predefined maximum value $P_{\max}$,

$$P = \sum_{k}^{M} a_k n_k \leq P_{\max}. \tag{43}$$

Here, k denotes the vibrational mode number, n_k is the quantum number of the primitive function for the kth mode, and a_k is the polyad coefficient. The latter can be estimated as

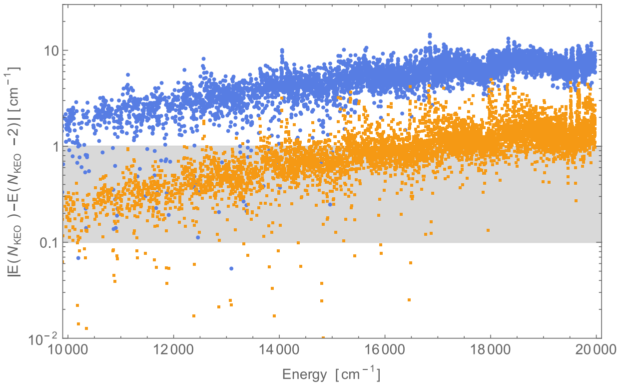

FIG. 4. Proof of convergence of KEO power series expansion for highly excited vibrational energies of NH_3. The absolute values for energy differences $|E(N_{\mathrm{KEO}})-E(N_{\mathrm{KEO}}-2)|$ are drawn for series truncation orders $N_{\mathrm{KEO}}=6$ and 8 in blue circles and orange squares, respectively.

$a_k = \omega_k / \min(\omega_1, \ldots, \omega_M)$, where ω_k denotes harmonic frequency of the kth vibrational mode. In all tests, unless stated, the KEO and PES were truncated after the 8th-order terms and the vibrational basis sets were truncated at the polyad numbers $P_{\max}$ = 32, 20, 16, and 12 for NH_3, PH_3, H_2CO, and CH_3Cl, respectively. All calculations were done variationally using the methods implemented in the computer program TROVE.

To investigate the error introduced by the power series truncation of the KEO, we performed a number of variational calculations of vibrational energies for different truncation orders N_{KEO}. The results are shown in Figure 1 for NH_3,

TABLE III. Basis set convergence of the $J = 5$ rotational energy levels for several fundamental bands of PH_3 obtained with three different molecule-fixed frames (see text). The energy differences $\Delta E(P_{\max}) = E(P_{\max}) - E(P_{\max} - 2)$ (in 10^{-3} cm^{-1}) are listed for two basis sets truncated at polyad numbers $P_{\max} = 10$ and 12. For visualisation purposes, the corresponding basis set errors in the band centres are subtracted from each rotational level.

					Eckart		Z-matrix		PAS	
Band	Sym	K_a	τ_{rot}	E_{12}/cm^{-1}	$\Delta E(10)$	$\Delta E(12)$	$\Delta E(10)$	$\Delta E(12)$	$\Delta E(10)$	$\Delta E(12)$
ν_2	E	5	0	1112.0689	1.4	0.1	−49.5	−6.3	−158.4	−21.1
	E	4	1	1115.0384	1.2	0.2	−57.5	−7.3	−103.2	−13.4
	A_2	3	1	1117.3652	1.0	0.2	−64.8	−8.2	−62.0	−7.8
	A_1	3	0	1117.3656	1.0	0.2	−64.5	−8.1	−62.0	−7.8
	E	2	0	1119.0361	0.8	0.2	−67.9	−8.5	−34.5	−4.1
	E	1	0	1120.0417	0.8	0.2	−52.7	−8.8	−19.4	−2.5
	A_2	0	1	1120.3774	0.7	0.2	−76.1	−9.5	−15.2	−1.6
ν_4	A_1	5	0	1220.4685	0.3	0.1	−43.7	−4.9	−149.7	−17.9
	A_2	5	1	1220.4685	0.3	0.1	−43.7	−4.9	−149.7	−17.9
	E	4	0	1229.9889	0.0	0.0	−42.2	−4.8	−94.4	−11.1
	E	3	0	1238.0712	−0.2	0.0	−41.7	−4.8	−56.3	−6.5
	A_1	2	0	1244.7297	−0.3	0.0	−41.7	−4.8	−32.3	−3.7
	A_2	2	1	1244.7622	−0.3	0.0	−41.4	−4.8	−32.5	−3.8
	E	1	1	1249.9960	−0.3	0.0	−33.0	−4.6	−20.2	−2.4
	E	0	1	1253.6712	−0.1	0.0	−32.9	−4.2	−16.0	−2.1
	A_1	1	0	1255.1494	0.1	0.0	−39.6	−4.6	−18.3	−2.1
	E	5	0	1256.3706	0.4	0.0	−40.9	−4.7	−193.1	−24.8
	A_2	4	1	1258.8342	0.1	0.0	−41.2	−4.8	−119.5	−15.1
	A_1	4	0	1258.8536	0.1	0.0	−40.8	−4.7	−120.9	−15.3
	E	3	0	1260.0959	−0.3	0.0	−40.4	−4.8	−49.9	−7.1
	A_2	1	1	1260.1336	−0.9	−0.1	−47.6	−5.3	−55.0	−3.0
	E	2	0	1260.3151	−0.6	0.0	−37.7	−4.5	−33.7	−5.5
ν_1	A_1	1	1	2458.5414	−0.1	1.0	−24.5	−1.5	−10.2	−0.6
	E	0	1	2459.0562	2.3	0.8	−24.1	−2.4	−70.2	−11.3
	A_1	2	1	2457.3137	−4.2	1.0	−29.3	−2.1	−47.4	−7.0
	E	1	0	2458.6973	−0.1	1.0	−37.0	−2.4	−10.4	−0.4
	A_2	1	0	2458.2820	−1.3	1.0	−28.7	−2.1	−28.4	−3.8
	E	2	0	2456.7709	−7.0	1.2	−35.1	−1.9	−24.7	−2.3
	A_2	2	0	2457.3791	−1.3	1.0	−28.7	−2.1	−28.3	−3.8
	E	3	1	2455.0033	−7.0	1.2	−34.4	−1.9	−24.7	−2.2
ν_3	E	3	1	2455.0033	8.5	0.5	−6.8	−3.7	−31.8	−12.4
	E	3	0	2454.1416	8.4	0.2	−4.2	−4.1	−24.8	−8.6
	A_2	5	0	2447.2150	0.3	0.5	−8.2	−4.4	−6.2	−1.4
	A_1	5	1	2447.2150	0.6	0.5	−8.2	−4.1	−9.7	−2.5
	A_2	4	0	2450.5003	1.2	0.4	−8.0	−4.2	−17.8	−5.1
	A_1	4	1	2450.5004	1.2	0.4	−8.3	−4.2	−17.8	−5.1
	E	4	0	2451.6983	2.5	0.5	−10.9	−3.7	−57.4	−15.2
	E	5	1	2445.8375	−0.2	0.4	−7.2	−4.3	−5.4	−1.2
	E	2	1	2451.0054	1.7	0.6	−8.7	−4.0	−15.2	−4.6
	E	4	1	2444.7540	−0.3	0.4	−8.7	−4.2	−5.6	−0.9
	A_2	3	1	2448.4773	0.6	0.5	−8.8	−4.2	−9.7	−2.4
	A_1	3	0	2448.4776	0.6	0.4	−7.7	−4.3	−9.4	−2.6
	E	1	0	2452.6351	3.7	0.6	−8.7	−3.8	−22.9	−7.9
	A_2	0	1	2453.1659	8.4	0.2	−4.1	−4.1	−24.8	−8.6
	E	5	1	2440.1378	−0.3	0.4	−8.4	−4.1	−6.6	−1.1

PH_3, and H_2CO as differences between energies calculated with KEO truncated at N_{KEO} and $N_{\mathrm{KEO}} - 2$ for $N_{\mathrm{KEO}} = 6$ and 8. For semi-rigid molecules, like PH_3 and H_2CO, the KEO expansion converges significantly faster when employing the linearized coordinates, as compared with the curvilinear ones. This is perhaps due to the fact that linearized coordinates are linear combinations of Cartesian coordinates, and therefore the KEO expressed in linearized coordinates can have a much simpler form than in curvilinear coordinates. An interesting observation is that for the non-rigid NH_3 molecule, both linearized and curvilinear representations converge at comparable rates being even more systematic in curvilinear coordinates. The reason is that for a non-rigid molecule the wavefunctions are more delocalized among the vibrational coordinates, making the contributions from the KEO high-order expansion terms more significant. Figure shows that convergence of the KEO expansion in curvilinear coordinates is improved by approximately one order of magnitude going from $N_{\mathrm{KEO}} = 4$ to 6 and from 6 to 8, thus convergence to within an error of about 0.01 cm^{-1} for vibrational energies below 10 000 cm^{-1} is obtained if series are truncated after 8th to 10th-order terms.

One of the main advantages of curvilinear coordinates is that they are very well adapted to represent the PESs, which is demonstrated in Figure 2, where the results of convergence tests for a power series expansion of the PES are shown for NH_3 and PH_3. As expected, the convergence of the PES expansion in linearized coordinates is poor and to reduce the error in the vibrational energies to about 0.1 cm^{-1} the expansion must be extended to include terms beyond 10th order. Since the original PESs are defined as 8th-order expansions in terms of the same curvilinear coordinates as employed in the present variational calculations, the results in Figure 2 for curvilinear coordinates converge exactly after the 8th-order terms.

More challenging is the basis set convergence, as it appears to be the main performance bottleneck of the variational method, essential for applications to larger molecules. Using two choices of internal coordinates, Figure 3 shows the differences between vibrational energies below 8000 cm^{-1} (4000 cm^{-1} for CH_3Cl) calculated with the basis sets truncated at polyad numbers $P_{\max}$ and $P_{\max} - 2$ ($P_{\max} - 4$ for NH_3) for several increasing values of $P_{\max}$. The results obtained with the curvilinear internal coordinates exhibit smoother and greatly accelerated basis set convergence compared to the linearized coordinates.

To test our new method, in Tables I and II we compare vibrational energies of NH_3 and H_2CO calculated in the present work with those from previous highly accurate theoretical studies[5,9] using the discrete representation approach and utilizing the same PESs.[87,89] In our calculations, the expansions of the KEO and PES were truncated after the 8th-order terms and the maximal for the present study vibrational basis sets, truncated at the polyad numbers $P_{\max} = 32$ for NH_3 and $P_{\max} = 16$ for H_2CO, were utilized. Evidently there is a very good agreement with previous results, within the claimed convergence uncertainties of 0.05 cm^{-1} for NH_3[5] and 0.005 cm^{-1} for H_2CO[9] for curvilinear coordinates and some larger deviations for linearized coordinates, which are most likely caused by the basis set incompleteness error.

For NH_3 as one of the most important spectroscopic species, we tested the ultimate accuracy one can achieve using the present approach for highly excited vibrational energy levels. Figure 4 depicts the results of convergence tests for expansion of the KEO of NH_3 in the high-energy region between 10 000 and 20 000 cm^{-1}. It is clearly seen that most of energy levels below 15 000 cm^{-1} are converged to better than 0.1 cm^{-1}, while the accuracy better than 1 cm^{-1} is achieved for the higher region up to 20 000 cm^{-1}. For comparison, the discrepancies resulting from the truncation of the KEO expansion are much smaller even than the errors inherited from the very accurate *ab initio* calculation[96] or spectroscopic refinement[86] of the PES for NH_3.

Finally, we investigate the effect of embedding, chosen for the body-fixed frame, on the basis set convergence of the excited rotational states. For our test we have chosen the asymmetric top PH_3 molecule and computed ro-vibrational energy levels for the following frame embeddings: (i) frame defined by the Eckart conditions (Eq. (9)); (ii) frame defined by the PAS conditions (Eq. (11)); (iii) Z-matrix frame that coincides with PAS at equilibrium, where the z-axis is aligned along the trisector while the x-axis lies along the projection of PH_1 bond on a plane perpendicular to the z-axis. The Eckart and Z-matrix frame embeddings were defined with respect to the C_{3v} reference structure. Table III compares the results for three choices of frame embeddings, where the energy variations (in 10^{-3} cm^{-1}) with respect to an increase of the basis set size from $P_{\max} = 8$ to $P_{\max} = 12$ are listed. To estimate the convergence of the rotational pattern within each vibrational band, the corresponding basis set errors in the vibrational band centers were subtracted from each rotational level. Evidently, the Eckart frame embedding shows the most consistent and quick convergence, however, as it was demonstrated by Szidarovszky *et al.*[52] for the H_2O molecule, the performance of the Eckart frame embedding may deteriorate for nuclear motion beyond the normal range, e.g., for high vibrational and rotational excitations associated with the tunnelling between several minima. For H_2O in particular, due to the relatively low barrier to linearity, the Eckart frame solution appropriate for nonlinear equilibrium structure breaks down when the molecule becomes linear.

VI. CONCLUSIONS

In this paper, we propose and numerically test a new fully automatic computational methodology for constructing a power series expansion of the Eckart-frame ro-vibrational Hamiltonian applicable to an arbitrary molecule and user-defined internal coordinates. Some flexibility to choose or implement other body-fixed frame embeddings, such as PAS embedding, is also provided. The method employs the automatic differentiation technique combined with a new method to solve and power-expand the Eckart frame equations. It is capable of precisely computing the Eckart-frame KEO expansion coefficients, even for high expansion orders, with accuracy comparable to that of symbolic differentiation but avoiding cumbersome analytic derivations. The method is implemented as part of the general variational approach TROVE.

The flexibility to employ different physically meaningful internal coordinates and body-fixed frames for different molecules, rather than to bias in favour of simplicity of the resulting KEO, is essential to be able to reduce the computational scaling of the variational solutions for medium-sized and larger systems. While there is at least one general implementation based on the discrete representation of the ro-vibrational Hamiltonian,[5] our previous power series expansion approach[3] lags behind in its flexibility to employ curvilinear internal coordinates. The limitations were associated with the accumulation of the round-off errors caused by the finite-difference differentiation as well as an unstable numerical approach for solution of the Eckart frame equations. These restricted the capacity of the method to construct high-order expansions in terms of curvilinear coordinates in favour of more facile linearized or normal coordinates. The present approach fully resolves these issues. The method, however, inherits some bottlenecks associated with the power series representation itself, such as series truncation errors and the need for essentially very high-order expansions if a non-rigid molecule is concerned. To some extent, the difficulties with non-rigid molecules can be avoided by utilizing the non-rigid Hamiltonian model,[95] that replaces the expansion along the large-amplitude vibrational mode by a discrete representation on a grid. For semi-rigid molecules, the series truncation can induce sizeable errors for high energy levels, though in our tests for a number of medium-size molecules such errors did not exceed a few 0.1 cm^{-1} for energies around 10 000 cm^{-1} when expansions truncated after the 8th-order terms were employed. For NH_3 in particular, we have showed that accuracy better than 0.1 cm^{-1} and 1 cm^{-1} can be obtained for energy levels below 15 000 cm^{-1} and 20 000 cm^{-1}, respectively, if the underlying KEO is expanded up to the 8th order. We believe that for medium-sized and larger molecules, the uncertainties in such high energy predictions will be mainly dominated by much larger basis set truncation errors and those caused by the limited accuracy of the underlying *ab initio* or spectroscopically refined PESs.

We conclude with comments on the significance of exploiting the curvilinear coordinates and the Eckart frame for power series expansion of the KEO. First, we have examined the performance of two internal coordinate models associated with the choice of curvilinear and linearized coordinates. We have shown that the linearized coordinates are more appropriate for expansion of the KEO of a semi-rigid molecule, whereas the curvilinear coordinates are more natural for compact representation of the PES and, more importantly, considerably improve the basis set convergence of the variational results. Second, we have assessed the effect of the body-fixed frame embedding on the basis set convergence of the rotationally excited states. As a test case, we performed variational calculations of the ro-vibrational energy levels of the PH_3 molecule employing three different body-fixed frame embeddings, two of which are "traditional" and one is due to the Eckart conditions. As expected, the results obtained with the Eckart frame show more quicker and regular convergence toward the complete basis set limit.

ACKNOWLEDGMENTS

We thank K. Chubb and J. Tennyson for critically reading the manuscript and suggesting improvements. We gratefully acknowledge the support from the ERC Advanced Investigator Project No. 267219 and the FP7-MC-IEF Project No. 629237. We also thank UCL for use of the Legion High Performance Computer and DiRAC@Darwin HPC cluster. DiRAC is the UK HPC facility for particle physics, astrophysics, and cosmology and is supported by STFC and BIS.

[1] D. Luckhaus, J. Chem. Phys. **113**, 1329 (2000).
[2] D. Lauvergnat and A. Nauts, J. Chem. Phys. **116**, 8560 (2002).
[3] S. N. Yurchenko, W. Thiel, and P. Jensen, J. Mol. Spectrosc. **245**, 126 (2007).
[4] E. Mátyus, G. Czakó, B. T. Sutcliffe, and A. G. Császár, J. Chem. Phys. **127**, 084102 (2007).
[5] E. Mátyus, G. Czakó, and A. G. Császár, J. Chem. Phys. **130**, 134112 (2009).
[6] E. Mátyus, J. Šimunek, and A. G. Császár, J. Chem. Phys. **131**, 074106 (2009).
[7] X.-G. Wang and T. Carrington, Jr., J. Chem. Phys. **130**, 094101 (2009).
[8] G. Avila and T. Carrington, Jr., J. Chem. Phys. **134**, 054126 (2011).
[9] G. Avila and T. Carrington, Jr., J. Chem. Phys. **139**, 134114 (2013).
[10] X.-G. Wang and T. Carrington, Jr., J. Chem. Phys. **138**, 104106 (2013).
[11] O. L. Polyansky, I. N. Kozin, R. I. Ovsyannikov, P. Malyszek, J. Koput, J. Tennyson, and S. N. Yurchenko, J. Phys. Chem. A **117**, 7367 (2013).
[12] A. V. Nikitin, M. Rey, and V. G. Tyuterev, J. Mol. Spectrosc. **305**, 40 (2014).
[13] A. F. Al-Refaie, A. Yachmenev, S. N. Yurchenko, and J. Tennyson, Mon. Not. R. Astron. Soc. **448**, 1704 (2015).
[14] C. Sousa-Silva, N. Hesketh, S. N. Yurchenko, C. Hill, and J. Tennyson, J. Quant. Spectrosc. Radiat. Transfer **142**, 66 (2014).
[15] X. Huang, R. R. Gamache, R. S. Freedman, D. W. Schwenke, and T. J. Lee, J. Quant. Spectrosc. Radiat. Transfer **147**, 134 (2014).
[16] X. Huang, D. W. Schwenke, and T. J. Lee, J. Chem. Phys. **140**, 114311 (2014).
[17] K. M. Dunn, J. E. Boggs, and P. Pulay, J. Chem. Phys. **86**, 5088 (1987).
[18] S. Carter, A. R. Sharma, and J. M. Bowman, J. Chem. Phys. **137**, 154301 (2012).
[19] M. Rey, A. V. Nikitin, and V. G. Tyuterev, Phys. Chem. Chem. Phys. **15**, 10049 (2013).
[20] S. N. Yurchenko and J. Tennyson, Mon. Not. R. Astron. Soc. **440**, 1649 (2014).
[21] T. Delahaye, A. Nikitin, M. Rey, P. G. Szalay, and V. G. Tyuterev, J. Chem. Phys. **141**, 104301 (2014).
[22] A. I. Pavlyuchko, S. N. Yurchenko, and J. Tennyson, "ExoMol molecular line lists: XI The spectrum of nitric acid," Mon. Not. R. Astron. Soc. (in press).
[23] A. V. Nikitin, M. Rey, and V. G. Tyuterev, J. Chem. Phys. **142**, 094118 (2015).
[24] C. Fábri, T. Furtenbacher, and A. G. Császár, Mol. Phys. **112**, 2462 (2015).
[25] J. K. G. Watson, Mol. Phys. **15**, 479 (1968).
[26] J. K. G. Watson, Mol. Phys. **19**, 465 (1970).
[27] J. M. Bowman, T. Carrington, and H.-D. Meyer, Mol. Phys. **106**, 2145 (2008).
[28] J. Tennyson and B. T. Sutcliffe, J. Chem. Phys. **77**, 4061 (1982).
[29] P. Jensen, J. Mol. Spectrosc. **128**, 478 (1988).
[30] A. G. Császár and N. C. Handy, J. Chem. Phys. **102**, 3962 (1995).
[31] M. J. Bramley and T. Carrington, Jr., J. Chem. Phys. **99**, 8519 (1993).
[32] L. Halonen, J. Chem. Phys. **106**, 831 (1997).
[33] M. Mladenovic, J. Chem. Phys. **112**, 1070 (2000).
[34] M. Mladenović, Spectrochim. Acta, Part A **58**, 795 (2002).
[35] D. Schwenke, J. Chem. Phys. **118**, 10431 (2003).
[36] T. Rajamaki, A. Miani, and L. Halonen, J. Chem. Phys. **118**, 6358 (2003).
[37] J. Tennyson, M. A. Kostin, P. Barletta, G. J. Harris, J. Ramanlal, O. L. Polyansky, and N. F. Zobov, Comput. Phys. Commun. **163**, 85 (2004).
[38] I. N. Kozin, M. M. Law, J. Tennyson, and J. M. Hutson, Comput. Phys. Commun. **163**, 117 (2004).
[39] X.-G. Wang and T. Carrington, Jr., J. Chem. Phys. **121**, 2937 (2004).
[40] F. Gatti and C. Iung, Phys. Rep. **484**, 1 (2009).
[41] M. Rey, A. V. Nikitin, and V. G. Tyuterev, J. Chem. Phys. **136**, 244106 (2012).
[42] M. H. Beck, A. Jäckle, G. A. Worth, and H.-D. Meyer, Phys. Rep. **324**, 1 (2000).
[43] D. Lauvergnat and A. Nauts, Chem. Phys. **305**, 105 (2004).
[44] H. G. Yu and J. T. Muckerman, J. Mol. Spectrosc. **214**, 11 (2002).
[45] J. M. Bowman, S. Carter, and X. C. Huang, Int. Rev. Phys. Chem. **22**, 533 (2003).

[46] Y. Scribano, D. M. Lauvergnat, and D. M. Benoit, J. Chem. Phys. **133**, 094103 (2010).
[47] C. Eckart, Phys. Rev. **47**, 552 (1935).
[48] J. D. Louck and H. W. Galbraith, Rev. Mod. Phys. **48**, 69 (1976).
[49] F. Wang, F. R. W. McCourt, and E. I. von Nagy-Felsobuki, J. Mol. Struct.: THEOCHEM **497**, 227 (2000).
[50] A. Čejchan and V. Spirko, J. Mol. Spectrosc. **217**, 142 (2003).
[51] S. N. Yurchenko, R. J. Barber, A. Yachmenev, W. Thiel, P. Jensen, and J. Tennyson, J. Phys. Chem. **43**, 11845 (2009).
[52] T. Szidarovszky, C. Fábri, and A. G. Császár, J. Chem. Phys. **136**, 174112 (2012).
[53] C. Fábri, E. Mátyus, and A. G. Császár, Spectrochim. Acta A **119**, 84 (2014).
[54] H. Wei and T. Carrington, Jr., Chem. Phys. Lett. **287**, 289 (1998).
[55] C. R. le Sueur, S. Miller, J. Tennyson, and B. T. Sutcliffe, Mol. Phys. **76**, 1147 (1992).
[56] J. M. Luis, M. Duran, J. L. Andrés, B. Champagne, and B. Kirtman, J. Chem. Phys. **111**, 875 (1999).
[57] P. R. Bunker and P. Jensen, *Molecular Symmetry and Spectroscopy*, 2nd ed. (NRC Research Press, Ottawa, 1998).
[58] H. Wei and T. Carrington, Jr., J. Chem. Phys. **107**, 2813 (1997).
[59] H. Wei, J. Chem. Phys. **118**, 7202 (2003).
[60] H. M. Pickett and H. L. Strauss, J. Am. Chem. Soc. **92**, 7281 (1970).
[61] A. Y. Dymarsky and K. N. Kudin, J. Chem. Phys. **122**, 124103 (2005).
[62] S. V. Krasnoshchekov, E. V. Isayeva, and N. F. Stepanov, J. Chem. Phys. **140**, 154104 (2014).
[63] J. Pesonen, J. Chem. Phys. **140**, 074101 (2014).
[64] V. Szalay, J. Chem. Phys. **140**, 234107 (2014).
[65] V. Szalay, J. Chem. Phys. **142**, 174107 (2015).
[66] K. Sadri, D. Lauvergnat, F. Gatti, and H.-D. Meyer, J. Chem. Phys. **141**, 114101 (2014).
[67] S. A. Smolyak, Sov. Math. Dosl. **4**, 240 (1963).
[68] E. Novak and K. Ritter, Numer. Math. **75**, 79 (1996).
[69] G. W. Wasilkowski and H. Woniakowski, J. Complexity **11**, 1 (1995).
[70] H.-J. Bungartz and M. Griebel, Acta Numerica **13**, 147269 (2004).
[71] G. Avila and T. Carrington, Jr., J. Chem. Phys. **135**, 064101 (2011).
[72] G. Avila and T. Carrington, Jr., J. Chem. Phys. **134**, 054126 (2011).
[73] D. Lauvergnat and A. Nauts, Phys. Chem. Chem. Phys. **12**, 8405 (2010).
[74] J. I. Rodriguez, D. C. Thompson, P. W. Ayers, and A. Koester, J. Chem. Phys. **128**, 224103 (2008).
[75] S. N. Yurchenko, M. Carvajal, P. Jensen, H. Lin, J. J. Zheng, and W. Thiel, Mol. Phys. **103**, 359 (2005).
[76] A. I. Pavlyuchko, S. N. Yurchenko, and J. Tennyson, "Hybrid variation-perturbation method for calculating rovibrational energy levels of polyatomic molecules," Mol. Phys. (in press).
[77] A. Griewank, in *Mathematical Programming*, edited by M. Iri and K. Tanabe (Kluwer Academic Publishers, Dordrecht, 1989), pp. 83–108.
[78] A. Griewank and A. Walther, *Evaluating Derivatives: Principles and Techniques of Algorithmic Differentiation*, 2nd ed. (SIAM, Philadelphia, PA, 2008).
[79] G. O. Sørensen, in *Large Amplitude Motion in Molecules II*, Topics in Current Chemistry, edited by M. J. Krische *et al.* (Springer, Berlin Heidelberg, Heidelberg, 1979), Vol. 82, pp. 97–175.
[80] M. Hardy, Electron. J. Combinatorics **13**, #R1 (2006).
[81] J. M. McCarthy, *Introduction to Theoretical Kinematics*, 2nd ed. (MIT Press, Cambridge, MA, 1990).
[82] C. Moler and C. Van Loan, SIAM Rev. **45**, 3 (2003).
[83] S. N. Yurchenko, W. Thiel, M. Carvajal, H. Lin, and P. Jensen, Adv. Quantum Chem. **48**, 209 (2005).
[84] S. N. Yurchenko, W. Thiel, M. Carvajal, and P. Jensen, Chem. Phys. **346**, 146 (2008).
[85] A. Yachmenev, S. N. Yurchenko, I. Paidarova, P. Jensen, W. Thiel, and S. P. A. Sauer, J. Chem. Phys. **132**, 114305 (2010).
[86] S. N. Yurchenko, R. J. Barber, A. Yachmenev, W. Thiel, P. Jensen, and J. Tennyson, J. Phys. Chem. A **113**, 11845 (2009).
[87] S. N. Yurchenko, J. Zheng, H. Lin, P. Jensen, and W. Thiel, J. Chem. Phys. **123**, 134308 (2005).
[88] C. Sousa-Silva, S. N. Yurchenko, and J. Tennyson, J. Mol. Spectrosc. **288**, 28 (2013).
[89] J. M. L. Martin, T. J. Lee, and P. R. Taylor, J. Mol. Spectrosc. **160**, 105 (1993).
[90] A. Owens, A. Yachmenev, S. N. Yurchenko, W. Thiel, and J. Tennyson, J. Chem. Phys. **142**, 244306 (2015).
[91] S. N. Yurchenko, R. J. Barber, and J. Tennyson, Mon. Not. R. Astron. Soc. **413**, 1828–1834 (2011).
[92] C. Sousa-Silva, A. F. Al-Refaie, J. Tennyson, and S. N. Yurchenko, Mon. Not. R. Astron. Soc. **446**, 2337 (2015).
[93] J. Tennyson and S. N. Yurchenko, Mon. Not. R. Astron. Soc. **425**, 21 (2012).
[94] A. Yachmenev, S. N. Yurchenko, P. Jensen, and W. Thiel, J. Chem. Phys. **134**, 244307 (2011).
[95] J. T. Hougen, P. R. Bunker, and J. W. C. Johns, J. Mol. Spectrosc. **34**, 136 (1970).
[96] X. Huang, D. W. Schwenke, and T. J. Lee, J. Chem. Phys. **134**, 044320 (2011).
[97] A. R. A. Derzi, T. Furtenbacher, J. Tennyson, S. N. Yurchenko, and A. G. Császár, J. Quant. Spectrosc. Radiat. Transfer **161**, 117 (2015).